RESEARCH ARTICLE

Investigation of the Effect of Reprocessing on Thermal and Mechanical Properties of Polymers and Polymer Nanocomposites

S. A. Vimukthi Dananjaya, Claudio Fortichiari, Yasith S. Perera, Chamila H. Dasanayaka, and Chamil Abeykoon*

This study explored the impact of multiple reprocessing cycles on the thermo-mechanical properties of polystyrene (PS) and low-density polyethylene (LDPE), simulated through reprocessing with a twin-screw extruder. Additionally, it compared the thermal and mechanical properties of graphene nanoplatelets (1% w/w) reinforced polypropylene (PP-GNP) nanocomposites with PP. The materials undergo seven consecutive extrusion cycles at varying screw speeds (100 and 150 rpm) and temperatures (180 and 200 °C). Increasing the screw speed from 100 to 150 rpm raised LDPE's screw torque by about 40% at the first reprocessing cycle. Processing PS at 200 °C reduced screw torque by ≈20% compared to 180 °C at 1–5 reprocessing cycles. Both torque and power decrease for PP and PP-GNP with each reprocessing cycle. LDPE's tensile modulus decreases with more cycles at 200 °C, while PS shows no consistent variation. PP's tensile modulus and ultimate tensile strength drop by 24% and 12%, respectively, from the first to the fifth cycle, while PP-GNP exhibits no consistent variation. Differential scanning calorimetry shows no clear change in LDPE's melting point, but an increase in PP and PP-GNP's melting points up to the fifth cycle. This research provides crucial insights to advance the recycling of polymers reducing environmental impact.

S. A. V. Dananjaya
School of Engineering
Swinburne University of Technology
Hawthorn, VIC 3122, Australia

C. Fortichiari, Y. S. Perera, C. Abeykoon
Northwest Composites Centre, Aerospace Research Institute, and
Department of Materials, Faculty of Science and Engineering
The University of Manchester
Oxford Road, Manchester M13 9PL, UK
E-mail: chamil.abeykoon@manchester.ac.uk

C. H. Dasanayaka
Institute of Business Industry and Leadership
University of Cumbria
Bowerham Rd, Lancaster LA1 3JD, UK

The ORCID identification number(s) for the author(s) of this article can be found under https://doi.org/10.1002/adem.202401260.

1. Introduction

Over the past few decades, the synthesis of polymers has considerably expanded and spread all over the world due to their excellent properties such as high specific strength, low cost, reproducibility, and ease of processing.[1–5] The term "plastics" refers to materials made up of polymers, a class of materials with a distinct set of chemical and physical properties, such as 1–90% chemical inertness, 1–50 mm yr^{-1} corrosion resistance, and 0.7–4.5 MPa fracture toughness, which can be attributed to their large molecular size. The combination of these favorable properties makes polymers ideal for countless applications spanning a variety of industries, such as packaging, household appliances, and electronics.[3,4,6–8] Among the most consumed plastics, polyethylene (PE), polypropylene (PP), and polystyrene (PS) play a major role, and they account for up to 44.8% of the global polymer market.[9]

Polymers are widely used in virgin, blend, and composite forms for numerous purposes according to the end application. Polymer nanocomposites, especially the ones produced through the incorporation of graphene nanoplatelets (GNP) into polymeric materials, are quite popular among those varieties due to their excellent properties, as reported in recent studies summarized in **Table 1**. The outcomes of these studies on GNP-polymer nanocomposites confirm the enhancement of a wide range of properties with the incorporation of GNP into polymeric materials. Moreover, it has been reported that the better intercalation and interface bonding of GNP with the polymer matrix,[10] good dispersion of GNP, and the high aspect ratio of GNP[11–14] lead to better reinforcement in GNP-based polymer nanocomposites. Since GNP-polymer nanocomposites are heterogeneous mixtures, composite processing methods such as solution blending,[15,16] in-situ polymerization,[17,18] and melt blending[19,20] are vital for ensuring the uniform dispersion of GNP in the polymer matrix. Although solution blending and in-situ polymerization result in better mixing of GNP with the polymer matrix,[10,19,21] they are not favorable for industrial manufacturing due to high production costs[22] and the use of hazardous chemicals.[23,24]

Despite their benefits, plastic products pose a significant threat to the environment and society, particularly when they

Table 1. A summary of recent studies on GNP-polymer nanocomposites.

Study	Composite Material	Objectives of the Study	Key Findings
Al-Saleh et al.[92]	PP-GNP nanocomposites	To prepare PP-GNP nanocomposites by adding compatibilizers using the melt compounding method. To investigate the effect of compatibilizers and GNP loading on the mechanical and thermal properties.	The tensile strength of 4 MPa of PP increasing from 1 to 5 wt% GNP loading, a slight increase in flexural strength and crystallinity of PP. The onset temperatures (T20% and T50%) of neat PP occurred at 291 and 317 °C, respectively, while with 1 to 5 wt% GNP loading, the values increased to 296–306 °C (T20%) and 322–346 °C (T50%), indicating improved thermal stability.
Botta et al.[120]	Biopolymer-based nanocomposites reinforced with GNP	To prepare and characterize GNP-filled biopolymer nanocomposites.	A 40% increase in Young's modulus with an increase in GNP loading from 0 to 5 wt%.
Narimissa et al.[121]	Biopolymer composites based on polylactic acid (PLA) and nano graphite platelets (NGP)	To develop and optimize PLA and NGP-based composites to achieve superior mechanical properties.	A 200% increase in Young's modulus with an increase from 0 to 3 wt% of GNP in the PLA matrix.
Gonçalves et al.[122]	Biocompatible reinforcement of PLA with GNP	To study the effect of mixing time, mixing intensity, and temperature during melt blending of GNP-filled PLA composites on their mechanical properties.	An increase of 12%, 20%, and 16% in Young's modulus, tensile strength, and elongation at break, respectively, in PLA nanocomposites.
Wang et al.[123]	Poly(sodium 4-styrenesulfonate) modified graphene for reinforced biodegradable poly(ε-caprolactone) nanocomposites	To improve graphene dispersion in poly(ε-caprolactone) to provide higher efficiency of reinforcement.	Both Young's modulus and elongation at break increased by 12% at 0.5 wt% GNP loading in poly(ε-caprolactone) nanocomposites.
Gao et al.[124]	PLA-GNP nanocomposites	To investigate the effect of particle size on mechanical, thermal, and electrical properties of PLA nanocomposites.	The Young's modulus of the PLA nanocomposite increased by 24% for large-size GNP and 10% for small-size GNP, respectively, at 5 wt% loading.
Cataldi et al.[125]	GNP-based advanced materials	To review the progress in GNP-based composite materials designed for flexible electronics, and motion and structural sensing.	Improved tensile properties after adding GNP into bio-composites.
Vallés et al.[126]	Few layer graphene-PP nanocomposites	To compare the mechanical properties of nanocomposites and balance the degree of functionalization to improve the compatibility of the matrix without aggregation.	A 200% increase in Young's modulus and a 10% increase in the degree of crystallinity with an increase of GNP (20 μm size) from 0 to 20 wt% in graphene-PP nanocomposites.
Carotenuto et al.[127]	Low-density polyethylene (LDPE) filled with graphite nanoplatelets	To investigate the effect of nanoscale reinforcement of graphite nanoplatelets within the LDPE matrix on the mechanical properties of the composite.	An improvement of 0.1 °C in the melting point and an increase of 100 MPa in the tensile strength was observed with an increase in the filler loading from 0 to 5 wt%.
Wang et al.[128]	Graphite nanosheets and carbon black as fillers for high-density polyethylene (HDPE)	To develop electrically conductive carbon fillers to be used in cables as semiconductive screens.	An increase of 2 MPa in Young's modulus and a slight increase in the crystallization temperature were observed, with an increase of 0 to 10 wt% of GNP in HDPE composites.
Sever et al.[129]	Expanded graphite/HDPE nanocomposites	To incorporate different-sized expanded graphite into HDPE and examine the electrical, mechanical, and structural properties.	An increase of 5 and 2200 MPa in the tensile strength and Young's modulus, respectively, and a 10^{15} Scm^{-1} electrical conductivity escalation were observed after adding 10 wt% graphite nanoparticles to HDPE composites.
Kalaitzidou et al.[130]	Multifunctional PP composites produced by incorporating exfoliated GNP	To explore the influence of GNP on the viscoelastic, barrier, and thermal properties of PP.	A six times larger thermal conductivity and a higher storage modulus were observed in 25 wt% GNP-filled PP compared to virgin PP.
Young et al.[14]	PP-GNP nanocomposites	To present a detailed analysis of the mechanism and mechanics of stress transfer in GNP-filled polymer matrices.	An increase of 50 MPa in Young's modulus with an increase from 0 to 10 vol% of GNP.
Pramoda et al.[10]	Covalent bonded polymer-GNP nanocomposites	To present an efficient and modern route of producing GNP/covalently-bonded-polymer nanocomposites and investigate their mechanical and thermal properties.	A higher Young's modulus and a storage modulus were observed with PMMA-GNP nanocomposites compared to PMMA-graphene oxide nanocomposites.
Ahmadi-Moghadam et al.[131]	Graphene/epoxy composites	To introduce a new method for GNP functionalization as a silane agent for improving reinforcement. To study and compare the structural, mechanical, and chemical properties of GNP-filled epoxy composites.	An increase of 38% and 14% in the tensile strength and Young's modulus, respectively, at 0.5 wt% GNP in epoxy.

Table 1. Continued.

Study	Composite Material	Objectives of the Study	Key Findings
Fayed et al.[132]	Electro-spun three-dimensional PS-GNP ultrafine fibril composite fabrics	To investigate the possibility of producing 3D GNP for ultrafine fibril composite fabrics and to study their morphological, mechanical, and thermal properties.	A 57% increase in the tensile strength at 10 wt% of GNP in ultrafine fibril composites.
Watt et al.[133]	Hybrid bio-composites from PP, sustainable biocarbon, and GNP	To study the influence of GNP addition on the mechanical, thermal, and morphological properties of compatibilized PP/bio carbon composites to determine the feasibility of using them in automotive applications.	An increase of 19% in the tensile strength, a 22% growth in Young's modulus, and a 17 °C improvement in the thermal stability were observed at 3 wt% GNP in Maleic anhydride grafted PP.
Lee et al.[134]	Polyurethane (PU) nanocomposites based on a highly concentrated graphite nanoplate/polyol masterbatch	To study the effect of GNP on the mechanical properties of composites. To examine the microphase separation inside the matrix.	An increase of 103% in the tensile strength and an increase of 152% in Young's modulus were observed at 0.1 wt% GNP in the PU nanocomposite.
Oyarzabal et al.[135]	bisphenol A polycarbonate/ graphene nanocomposites	To prepare polycarbonate/graphene nanocomposites with commercially available graphene (without any additional treatment) using a simple single melt mixing procedure.	An increase of 52% in Young's modulus was observed at 7 wt% GNP in the polycarbonate matrix.
Kiziltas et al.[136]	GNP reinforcement of bio-based polyamide nanocomposites for automotive applications	To investigate the effect of nanofillers on the electrical, rheological, morphological, thermal, and mechanical properties of the nanocomposites.	A 25% and 56% improvement in the tensile strength and Young's modulus, respectively, with 7 wt% GNP in the polyamide composite.
Hamidinejad et al.[137]	Polymer-GNP composites fabricated via supercritical-fluid treatment and physical foaming	To develop a facile, cost-effective, and industrially viable method to produce lightweight and conductive polymer-GNP nanocomposites.	A 404% increase in thermal conductivity was observed with 18 vol% GNP in HDPE polymer composites.
Yu et al.[138]	Thermally conductive composite film filled with highly dispersed GNP via the solvent-free one-step fabrication	To propose an application process for the one-step fabrication of high-conductivity polymer composite films based on the previously proposed processes of powder mixing and in situ polymerization.	The thermal conductivity increased by 857% at 20 wt% GNP in cyclin butylene terephthalate.
Araby et al.[139]	Electrically and thermally conductive elastomer/GNP nanocomposites by solution mixing	To find effective solution-mixing polymers with cost-effective graphene of hydrophobic surface for preventing the stacking of graphene layers.	The tensile strength, Young's modulus, thermal conductivity, and tear strength improved by 413%, 782%, 83%, and 709%, respectively, at 24 vol% GNP in styrene butadiene rubber.
Wijerathne et al.[140]	GNP-reinforced recycled polycarbonate composites	To broaden the understanding of the nanofiller reinforcement capability for improving the properties of recycled polycarbonate composites.	A 12 °C enhancement in the thermal stability and an increase of 72% in the failure strength of 10 wt% GNP in recycled polycarbonate/GNP composites were observed.
Qi et al.[141]	PS nanocomposites with ultralow graphene content	To enhance the conductivity of PS with ultra-low graphene content.	A 6.7×10^{-14} to 3.49 Sm^{-1} increase in the electrical conductivity was observed at 1.1 vol% GNP in PS.
Polschikov et al.[142]	PP-GNP nanocomposites	To examine the properties of isostatic PP filled with GNP produced by in-situ polymerization.	The crystallization and melting temperatures of 5.6 vol% GNP in isostatic PP increased by 16 and 4 °C, respectively.
Pereira et al.[143]	GNP-based multifunctional eco composites	To develop smart and multifunctional eco composites based on flax fabrics coated with optimized GNP polymeric formulations composed of chitosan and polyethylene glycol.	A 30 °C improvement in the degradation temperature of 2% GNP-filled polyethylene glycol.
Mayoral et al.[144]	Biaxially stretched PP-GNP composites	To explore the effects of the biaxial stretching action and the presence of filler materials on the resulting structure and the properties of stretched PP-GNP composites.	The degree of crystallization resulted from biaxial stretching, increased from ≈40% (unstretched) to ≈63% at 15 wt% GNP, and to ≈70% at 20 wt% GNP.
Al-Maqdasi et al.[145]	Wood and GNP-reinforced polymer composites	To produce a commercial masterbatch of GNPs in HDPE to enhance the physical and mechanical properties of wood flour-reinforced polymer composites. To demonstrate the synergistic effect of reinforcing the polymer with varying amounts of wood and GNPs.	The tensile stiffness, yield stress, impact strength, thermal conductivity, and diffusivity showed an increase of 140%, 79%, 35%, 80%, and 210%, respectively, with increasing GNP content up to 15 wt%.

near the end of their useful lives.[25,26] The consumption of plastic products and the resulting plastic waste continue to grow exponentially,[27] despite the recent demands and regulations to limit the manufacture of single-use/disposable plastic products. The organization of economic cooperation and development (OECD) recently signed a deal that is expected to spark a worldwide initiative to reduce the harmful effects of improper management of plastic waste. As of now, plastic waste is largely mismanaged worldwide, and finding ways to recuperate is still a complex and challenging problem.[28]
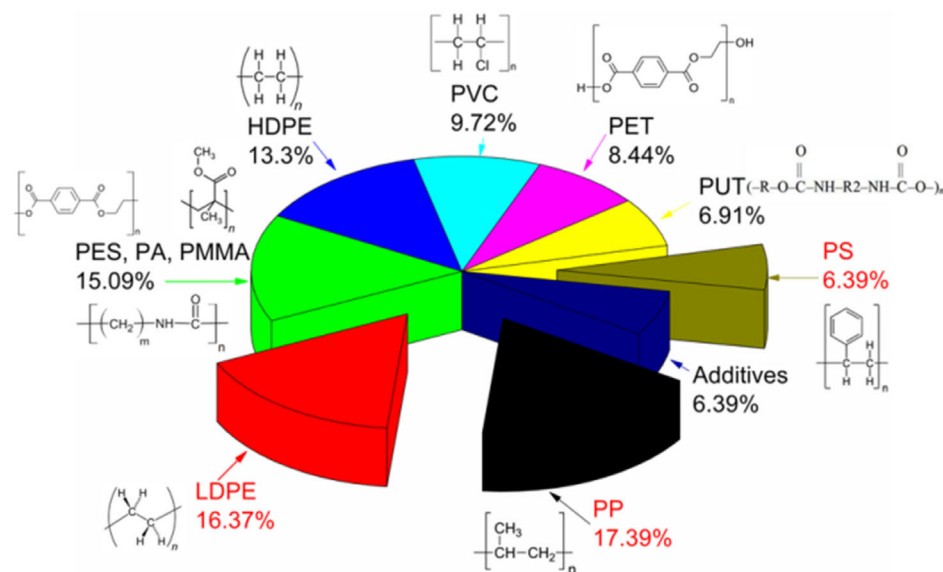
Figure 1. The global plastic waste generation in 2015. Reproduced with permission.[27] Copyright 2015, American Association for the Advancement of Science.

Figure 1 provides an outlook of the global plastic waste generation in 2015.[27]

As evident from Figure 1, PP and LDPE waste account for 17.39% and 16.37%, respectively, and are the two most dominant materials in the global plastic bin. At present, the most likely scenario, except for a handful of countries like Norway and Switzerland, for used or End-of-Life (EoL) plastics is to exit the lifecycle by being dumped in landfills, while virgin materials are used for new products.[29] The scene is more diversified with less indebted middle-income countries (LIMICs). According to Wilson et al.[30] about 2 billion people are left to manage their own municipal solid waste, primarily by scattering it on the ground, or more commonly by burning it in the open, which Lau et al.[31] estimated to be between 18 and 49 million tons of plastic waste annually. Waste pickers, which may number between 10 and 20 million,[30,31] are the primary source of material gathered for recycling in LIMICs.[32] Operations for sorting and recycling plastics are frequently smaller and, in some circumstances, poorly regulated, with no safeguards for the environment, workers' rights, or public health. A more far-sighted and efficient view is to introduce the waste materials back into the cycle by repurposing them, and this method is generally referred to as recycling.[33] This contributes to the idea of building a circular economy, where the lifecycle of materials for consumption is extended for as long as possible by sharing, reusing, and recycling to create further value out of materials and thereby minimizing the amount of waste generated.[34]

According to the OECD Global Plastics Outlook Database,[35] 50% of global plastic waste was landfilled in 2019, with mismanaged, incinerated, and recycled plastic waste accounting for 22%, 19%, and 9%, respectively, as shown in **Figure 2**. Recycling is currently the ideal solution for reintroducing consumed materials into the circular economy.[36,37] **Table 2** presents a summary of previous studies on polymer recycling and reprocessing.

Recycling techniques can be classified as thermal recycling,[38] feedstock recycling,[39] and thermomechanical recycling.[40]
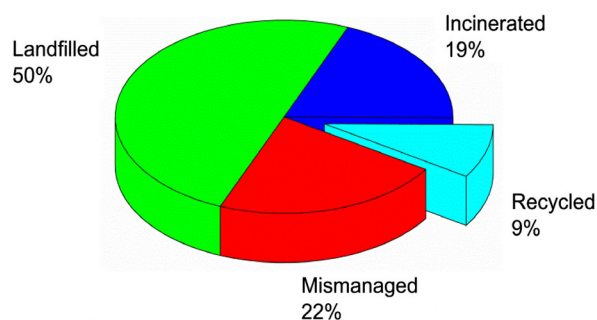
Figure 2. OECD Global Plastics Outlook Database. Reproduced with permission.[35] Copyright 2019, OECD.

Thermally recycled materials are not regenerated and are lost in a combustion reaction.[37] Feedstock recycling is not feasible and affordable.[37] However, this is more effective than landfilling[41] or incinerating[42] while also being more immediately applicable to a larger scale.[42] Among the recycling methods considered, thermomechanical recycling is designated as the technique with the most significant balance between technological preparedness and environmental advantage.[43]

For producing polymer composites, melt blending is more popular in the industry due to its scalability[44] and economic feasibility despite its drawbacks, such as the slightly lower aspect ratio[45] and the lower degree of dispersion in certain conditions.[46] Among the machinery used for melt blending, twin-screw extruders are commonly used to produce polymer nanocomposites.[47] Screw extrusion has become a mainstay for processing thermoplastic polymers and is one of the most prevalent processing methods among the different polymer processing techniques.[48,49]

Extrusion processing parameters such as the screw rotational speed, die and barrel set temperatures, cooling rate, and material feed rate have a significant influence on the stability of the extrusion process and the quality of the extruded product.[50–52]

Table 2. A summary of existing studies on plastic waste recycling and reprocessing.

Study	Application	Objectives of the Study	Key Findings
Wölfel et al.[146]	Recycling and reprocessing of thermoplastic PU materials toward nonwoven processing.	To study the basic raw material properties, morphological, mechanical, and thermal properties of reprocessed PU.	The molecular weight was reduced by 50% at the eighth run, and the crystallization enthalpy decreased by about 60%, approaching a minimum.
Jubinville et al.[43]	Thermomechanical recycling of PP for the facile and scalable fabrication of highly loaded wood plastic composites (WPCs).	To investigate the possibility of utilizing reprocessed and recycled PP, which generates altering degrees of degradation, to fabricate highly filled WPCs free of other lubricants and compatibilizers.	After six reprocessing cycles, PP's molecular weight and tensile strength reduced by 20.69% and 9.86%, respectively.
Aumnate et al.[65]	Recycling of PP/polyethylene (PE) blends: the effect of chain structure on the crystallization behaviors.	To study the influence of various chain structures of PEs on the crystallization behavior and tensile properties of PP/PE blends.	Crystallinity experienced a 20% reduction for LDPE and a 16% improvement for HDPE in PP blend up to 100 wt%. Tensile strength showed a 26% reduction up to 100 wt% LDPE.
Bataineh [147]	Life-cycle assessment of recycled postconsumer HDPE and polyethylene terephthalate (PET).	To measure the overall environmental performance of mechanical recycling of postconsumer HDPE and PET.	Recycled HDPE pellets required 12–13% energy in the cut-off recycling method, while 62% energy was consumed by the system expansion method.
Bumanis et al.[148]	Thermal and sound insulation properties of recycled expanded PS granule and gypsum composites.	To produce gypsum matrix composites filled with expanded PS waste as a lightweight aggregate prepared by traditional casting and semi-dry compression methods and evaluate the mechanical and thermal properties.	The thermal conductivity reduced from 0.079 to 0.039 $Wm^{-1}K^{-1}$) and the apparent density decreased from 298 to 48 kgm^{-3} with four times drop in the gypsum content.
Gandhi et al.[149]	Life cycle assessment of recycling HDPE waste.	To study the environmental burdens and energy consumption of different polymer processing steps within the mechanical recycling process.	Mechanical recycling of HDPE consumed 40% of the amount of energy consumed by other plastic recycling methods with less fossil fuel consumption.
Montava-Jorda et al.[150]	Mechanical recycling of partially bio-based and recycled PET blends by reactive extrusion with poly (styrene-co-glycidyl methacrylate).	To ascertain the possibility for mechanical recycling of the next generation PET materials using rheological, thermal, mechanical, and thermomechanical property characterization.	An increase of 303.1% and 368.8% in toughness at 3 Phr and 5 Phr of poly (styrene-co-glycidyl methacrylate) in PET, respectively.
García-Barrera et al.[151]	A recycling alternative for expanded PS residues using natural esters.	To provide a new eco-friendly recycling method for expanded PS.	Omega-3 dissolved expanded PS waste in 30 mins with a recovery of 94.6%, compared to glyceryl tributyrate, which took 130 mins with a recovery of 68.4%.
Alabi et al.[152]	Powder production from recycled LDPE waste and doum palm nuts for lightweight engineering applications.	To reduce plastic and agro-waste by recycling. To study the potential of doum palm nut and recycled waste LDPE as raw materials for lightweight structural engineering applications.	Recycled LDPE powder showed approximately an increase of 30 °C in thermal stability and an increase of 15 °C in the endothermic peak compared to doum palm nut powder.
Eriksen et al.[153]	Contamination in plastic recycling: Influence of metals on the quality of reprocessed plastics.	To obtain samples of PET, PE, PP, and PS plastic waste and reprocessed plastic waste (pellets or flakes) from households and investigate metal contamination levels and their potential effect on the applicability of reprocessed waste plastic in material recycling.	The concentrations of Al, Pb, Ti, and Zn metals in household waste were considerably larger than those of other types of waste and virgin plastics.
Tiancheng Wei et al.[154]	Progress of recycled polyester in rheological performance in moulding, and economic analysis of recycled fibers in fashion and textile industry	To evaluate the properties of polyester for durable and feasible end products.	Maximum shear viscosity was obtained at 15% additive loading.
Jin et al.[155]	Effect of extensive recycling on flow properties of LDPE	To modify the technological parameters during LDPE processing.	At 100 processing cycles, the melt flow index of LDPE was reduced from 23.1 to 0.2 g min^{-1}, with the insoluble fraction about 35 %.

ADVANCED
SCIENCE NEWS

www.advancedsciencenews.com

**ADVANCED
ENGINEERING
MATERIALS**

www.aem-journal.com

Table 2. Continued.

Study	Application	Objectives of the Study	Key Findings
Singh et al.[156]	Waste management by recycling of polymers with reinforcement of metal powder.	To perform recycling of waste plastics with the addition of Fe powder by controlling the melt flow index.	To improve mechanical properties, 90% HDPE + 10% Fe powder composite and the 100% LDPE are the most suitable compositions.
Zhang et al.[157]	Blending recycled HDPE with the virgin polymer as an effective approach to improve the mechanical properties.	To determine the influence of blending virgin and recycled polymers on both the tensile and fatigue properties. To compare the effects of different mixing approaches.	Regardless of the mixing method, virgin HDPE has a higher tensile strength than recycled HDPE.
Ramesh et al.[158]	Recycling of engineering plastics from waste electrical and electronic equipment: Influence of virgin polycarbonate and impact modifier on the final performance of blends.	To reutilize the ecological and economical engineering plastics with a melt blending technique, instead of open burning which causes environmental pollution.	Recycled plastics blended with 10% virgin polycarbonate showed a 167.7% increase in the impact strength and a 11 % improvement in the storage modulus.
Ragaert et al.[159]	Mechanical and chemical recycling of solid plastic waste.	To present a comprehensive description of thermal and mechanical recycling of plastics.	Mechanical recycling is economically more feasible and thermal recycling is unfavorable due to contamination, and both methods showed promising results compared to landfilling.

Gálvez et al.[53] studied the thermomechanical properties of PLA processed at 60 and 150 rpm rotational speeds at a 160 °C temperature and claimed that the polymer processed at 60 rpm exhibited better tensile and thermal properties. Feng et al.[54] observed a reduction in the viscosity when increasing the temperature from 150 to 170 °C at 35 rpm and concluded that the screw speed and melt temperature are directly related to the viscosity. While the polymer travels across an increasing temperature gradient, it continues to be sheared and mixed by the screw. Eventually, it is forced out of a die, which extrudes the polymer at a constant cross-section.[54] As a result of the shear forces in an extruder, polymer chains can experience severe degradation and changes in their chemical structure and molecular weight.[55] Generally, polymers are degraded by chain scission and crosslinking inside an extruder.[56] The former decreases the average molecular weight of the polymer, whereas the latter increases it.[57] Chain scission or cleavage is identified as the most common effect in PP, whilst crosslinking prevails in PE.[58] The differences in thermal degradation mechanisms were further studied by Scott et al.[59] through the observation of the mechanical properties of PE and PP. However, thermomechanical recycling needs further improvements for it to be capable of recovering more types of waste products and producing materials with smaller deterioration in properties.

The impact of recycling on the thermal, rheological, and mechanical characteristics of polymers has been the subject of numerous research works. In a previous study on the mechanical recycling of LDPE, Jin et al.[60] discovered that while chain crosslinking predominated overall, chain scission prevailed during the first extrusion cycle. According to Abad et al.[61] at the fifth reprocessing cycle, LDPE degraded by branching and crosslinking with an increase in the yield stress and Young's modulus and a significant decrease in failure stress, failure strain, and fracture energy. HDPE degrades primarily by chain scission. Aurrekoetxea et al.[62] found a linear increase in Young's modulus for the first eight cycles, at which point the modulus peaked. Huang et al.[63] and Incarnato et al.[64] investigated the effect of the number of recycling cycles on the properties of PP and found a decrease in the molecular weight and fluidity with an improvement in the crystallization rate. When comparing PP with HDPE, it was found that the rate of decrease in the molecular weight of PP was faster than that of HDPE. Moreover, blending LDPE into PP was found to reduce the overall crystallization rate.[65] Rust et al.[66] investigated the degradation of virgin and recycled isotactic PP from battery casings and confirmed that the reprocessing of PP led to the degradation of isotactic PP via chain-breaking mechanisms, resulting in a reduction in entanglements and tensile properties.

The main contribution of this study is to investigate the effect of reprocessing cycles on the thermomechanical properties of LDPE, PS, PP, and PP-GNP materials, and this is an area which has yet to be reported in the existing literature. Here, studying the effect of successive extrusion cycles on the properties of polymers can enhance our understanding of the methods and processing conditions that ought to be adopted during recycling and which conditions are favorable to prevent the degradation of their properties. The influence of polymer degradation within the context of thermomechanical recycling at three different processing conditions and seven processing cycles was also studied. Overall, this study extends the knowledge on reprocessing polymeric materials, which should be really helpful in reusing/reprocessing polymers and hence supporting circular economy.

2. Experimental Section

2.1. Materials

In this study, three polymeric materials (i.e., LDPE, PP, and PS) were used, the details of which are summarized in **Table 3**. The physical and mechanical properties of these polymers are

**ADVANCED
SCIENCE NEWS**

www.advancedsciencenews.com

**ADVANCED
ENGINEERING
MATERIALS**

www.aem-journal.com

Table 3. Physical properties of the polymers as per the manufacturers' datasheets.

Polymer	Brand name	Manufacturer	$\rho(gcm^{-3})$	$T_g(°C)$	$T_m(°C)$	Melt flow rate (MFR) [g/10 min]
LDPE	Lupolen 2420H	LyondellBasell	0.924	−120/−90	111	1.9
PP	SCG P739ET	SCG Chemicals	0.920	−10	175	55.0
PS	Styrolution PS 124N	Styrolution	1.040	101	−	−

provided in **Table** 3 and 4, respectively. To produce the PP-GNP nanocomposites, GNP with a particle size of 15 μm and a surface area of 120–150 m^2 g^{-1} were used.

2.2. Experimental Procedure

All raw materials were subjected to conditioning by exposing them to the standard atmospheric conditions in the laboratory for 24 h. After preheating the materials at 70 °C for 2 h, the materials were processed using a Thermo Scientific Haake PolyLab Rheomex parallel twin-screw extruder, which was equipped with a co-rotating twin-screw with a diameter of 16 mm and a length-to-diameter (L/D) ratio of 25:1. The extruder barrel was 400 mm long with 10 heaters installed along its length. Each heater had a rating of 300 W and 240 V. Three different processing conditions were used in the extruder during the experiments, as shown in **Table** 5, to assess the effect of the processing conditions on the materials during reprocessing.

Polymer pellets were fed at a constant rate into the extruder using a Brabender volumetric feeder. The extruded polymer was run through a water bath and fed into a Haake pelletizer, which chopped and pelletized the extruded polymer.

The PP-GNP nanocomposites were prepared through melt-mixing of GNP with molten PP in the twin-screw extruder. GNP (5 g) was added to 500 g of PP by feeding GNP to the extruder simultaneously with the polymer using a Brabender gravimetric feeder. The polymers and GNP were fed to the extruder at feed

Table 4. Mechanical properties of the polymers as per the manufacturers' datasheets.

Polymer	Tensile modulus [MPa]	Yield stress [MPa]	Ultimate tensile strength (UTS) [MPa]	Strain at break
LDPE	260	11	32-60	0.30
PP	1270	27	−	1.60
PS	3200	50	−	0.02

Table 5. Different processing conditions used in the extruder for processing the materials.

Processing condition	Screw speed [rpm]	Barrel set temperatures [°C]			
		Temperature condition	Zones 1–3	Zones 4–6	Zones 7–10
A	100	200	160	180	200
B	150	180	150	160	180
C	100				

rates of 960 and 50.53 g hr^{-1}, respectively. A Nederman extraction hood was used to extract airborne particles.

Figure 3 presents a schematic explaining the procedure for processing the materials. The pellets collected were transferred to a tray covered with aluminum foil. The tray was placed in a vacuum oven to remove the residue water and moisture absorbed from the water bath. Once dried, a sample of 30 g was taken for testing, and the rest of the material was fed back into the extruder for reprocessing. This procedure was repeated for seven processing cycles.

The feed rate of the volumetric feeder was set at 6% for the experimental sets running at 100 rpm (i.e., processing conditions A and C) and 9% for those running at 150 rpm (i.e., processing condition B), to ensure a linear relationship between the mass flow rate of the output and the screw speed. A temperature gradient was created inside the extruder by setting the temperatures of the barrel heaters, as indicated in Table 5.

During the experimental trials, the torque required to turn the screw, as well as the amount of power consumed by the extruder, were recorded. This was done to get an insight into the influence of different processing conditions, materials, and reprocessing cycles on the torque generation and power consumption of the extruder. The amount of power consumed by the extruder is affected by the torque and the rotational speed of the screw. (Also, the heat required to increase the temperature inside the extruder is a major method of power consumption). The torque required to turn the screw was recorded using a torque sensor integrated into the extruder system, which continuously measured the rotational resistance during operation. Their mathematical relationship is expressed by Equation (1) and (2), where P, T, ω, and n_{rpm} denote the power consumption, torque, angular velocity, and screw rotations per minute, respectively.

$$P = T\omega \tag{1}$$

$$P = T\frac{\pi n_{rpm}}{30} \tag{2}$$

2.3. Tensile and Thermal Testing

Bone-shaped tensile test specimens with dimensions of $4.9 \times 1.6 \times 50$ (mm in width x thickness x gauge length) were prepared using a Haake Minijet II micro-piston injection moulding machine with a barrel holding about 4 g of polymer. LDPE pellets were transferred into the heater to melt and then injected into the mold at 400 bar for 8 s and holding at 250 bar for 4 s. The injection moulding machine was kept at 200 °C and the mould at 40 °C. PS was injected at 550 bar for 6 s and then held at 300 bar for 5 s. For PS, the injection molding machine was at 200 °C, but the mold was
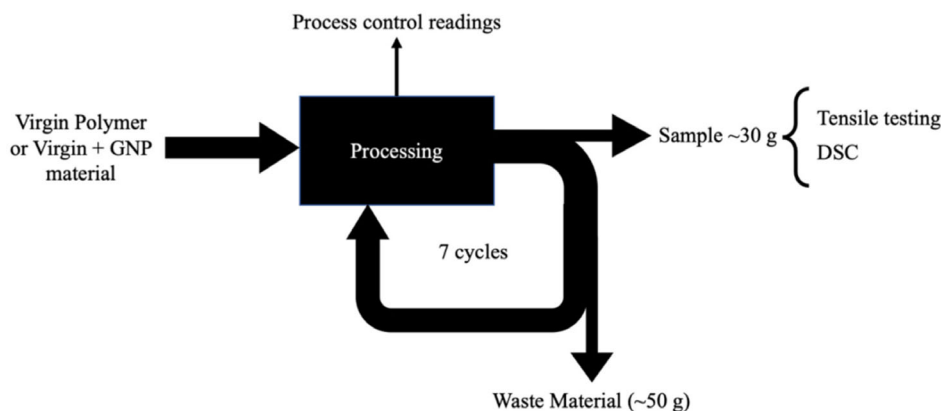
Figure 3. Flowchart of the procedure followed during the experiments.

kept at 65 °C, to allow easier detachment of the specimen. Five tensile specimens of each polymer sample were produced. All these set conditions were identified through trials carried out prior to proper tests and every sample test was replicated for three times.

Tensile tests were performed with a 500 N load cell for 60 s using an Instron tensile testing machine, following the ISO 527 standard with strain rates applied as shown in **Table 6**. While this variation in strain rates may hinder a direct comparison between the materials, it was essential to ensure a low signal-to-noise ratio across all tests.

Differential scanning calorimetry (DSC) was performed using 2 and 20 mg test samples with a TA Instruments Q1000 Thermal

Analyzer in the temperature range from 20 to 220 °C, at 10 °C min^{-1}, within an inert gas atmosphere around the sample.

3. Results and Discussion

3.1. Process Control Measurements

3.1.1. Process Control Measurements for LDPE

Figure 4 and **Table 7** display the average torque generation and power consumption of the extruder during reprocessing of LDPE under each processing condition. Processing LDPE at 150 rpm and 180 °C (i.e., processing condition B) resulted in the highest power consumption across all reprocessing cycles. Under this processing condition, the torque dropped by 28.7% from the first cycle to the third and by 17.8% from the sixth cycle to the seventh, while the torque rose by about 10% from the third cycle to the sixth. According to the Figure 4, large error bars could be visible at the first reprocessing cycle. Large error bars in the torque values during the first reading of extrusion could be due to material inconsistencies, such as uneven flow or poor initial mixing of the composite. Additionally, fluctuations in pressure at the start of the process can cause variations in the torque measurement.

Table 6. Strain rates applied during tensile tests for each polymeric material.

Polymer or matrix material	Strain rate [mm min^{-1}]
LDPE	25
PS	2
PP	100
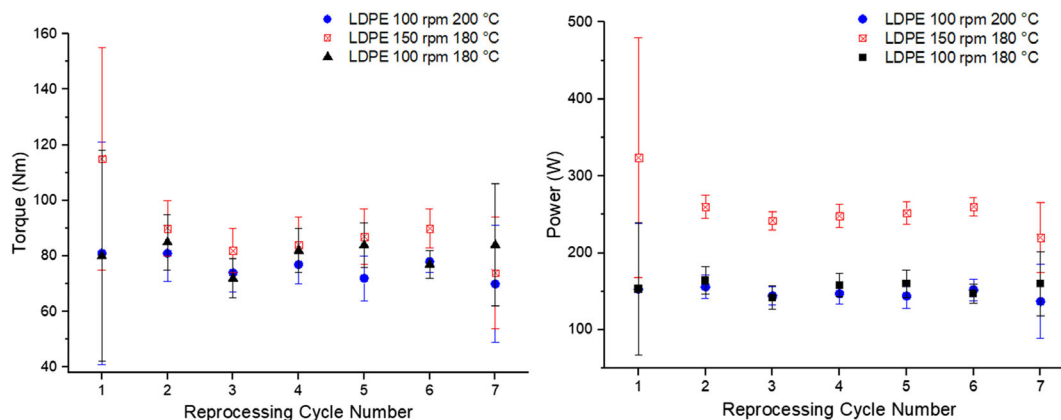
Figure 4. Variation of the average torque generation and power consumption of the extruder during reprocessing of LDPE under different processing conditions.

Table 7. Average torque generation and power consumption values of the extruder during reprocessing of LDPE under different processing conditions.

Reprocessing cycle	Average torque generation [Nm]			Average power consumption [W]		
	100 rpm 200 °C	150 rpm 180 °C	100 rpm 180 °C	100 rpm 200 °C	150 rpm 180 °C	100 rpm 180 °C
1	81	115	80	153	324	153
2	81	90	85	156	260	164
3	74	82	72	144	242	142
4	77	84	82	147	248	158
5	72	87	84	144	252	160
6	78	90	77	152	260	147
7	70	74	84	137	220	160

The decrease in torque could be due to the reduction in the viscosity of the polymer melt as a result of deterioration.[67] A fall in viscosity indicates that chain scission occurred during the reprocessing cycles 1 to 3 and 6 to 7.[68,69] This can be expected considering the results reported by Jin et al.[60] where chain scission was found to be the dominating mechanism during the first cycle. Khanam et al.[70] also identified a viscosity drop in LDPE-GNP nano-composites due to chain scission inside a twin-screw extruder. A similar finding on the viscosity drop in LDPE caused by chain scission inside a single-screw extruder was reported by Yamaguchi et al.[71] Castéran et al.[72] and Teymouri et al.[73] provided a detailed explanation of the chain scission of PE inside a twin-screw extruder, which caused a viscosity drop.

Between the third and sixth reprocessing cycles under processing condition B, crosslinking of the polymer might have occurred, which increased the viscosity of the polymer and, in turn, increased the torque and power.[74] Andersson et al.[75] identified an increase in the torque caused by the crosslinking of PE inside a twin-screw extruder. However, the increase in torque and power between the third and sixth reprocessing cycles is small and could have been caused by the uncertainty in the measurements. In that case, an overall downward trend in torque with

an increasing number of reprocessing cycles would signify a slow and steady reduction in molecular weight. It can be seen from Table 7 that processing LDPE at 150 rpm and 180 °C (i.e., processing condition B) resulted in higher torque generation compared to processing at 100 rpm and 180 °C (processing condition C). This is expected as processing at a higher screw speed shears the polymer melt at a higher rate, which in turn applies more mechanical resistance to the motion of the screw resulting in increased torque generation.[76,77] Abeykoon et al.[78] reported an increase of 80 Nm in torque with an increase in the screw speed from 10 to 90 rpm. However, the rate of increase of the torque reduced as the polymer's viscosity dropped due to shear thinning. Abeykoon et al.[52] reported a comparable result of increased torque resulting from an increase in the screw speed from 10 to 50 rpm during the processing of LDPE.

The power consumption exhibits a similar trend to the torque with an increasing number of reprocessing cycles under different processing conditions. The similarity between the behavior[79] as can be observed from Equation (1). There may be a difference occurred at the experimental values obtained than the theoretical values from Equation (1) and (2) due to the heat generation inside the extruder, energy losses and other variations of conditions. As evident from Figure 4 and Table 7, the power consumption is increased by a factor of more than 1.3 at all reprocessing cycles when the screw speed increased from 100 to 150 rpm, which can be attributed to the combined effect from the increased screw rotational speed as well as the increased torque caused by high shear rates.[80]

3.1.2. Process Control Measurements for PS

Figure 5 and **Table 8** present the average torque generation and power consumption of the extruder against the number of reprocessing cycles of PS under different processing conditions. The highest torque values were reported when the material was processed under processing conditions B and C, while the highest power consumption values were reported under processing condition B across all reprocessing cycles. Similar to the case of LDPE, the significantly large power consumption under
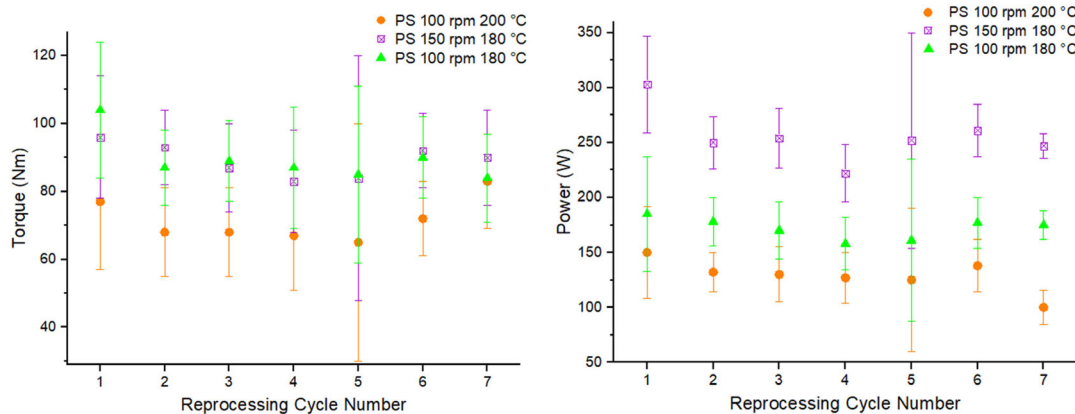
Figure 5. Variation of the average torque generation and power consumption of the extruder during reprocessing of PS under different processing conditions.
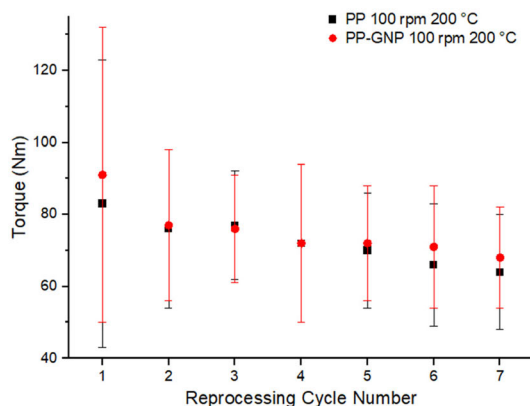
Table 8. Average torque generation and power consumption values of the extruder during reprocessing of PS under different processing conditions.

Reprocessing cycle	Average torque generation [Nm]			Average power consumption [W]		
	100 rpm 200 °C	150 rpm 180 °C	100 rpm 180 °C	100 rpm 200 °C	150 rpm 180 °C	100 rpm 180 °C
1	77	96	104	150	303	185
2	68	93	87	132	250	178
3	68	87	89	130	254	170
4	67	83	87	127	222	158
5	65	84	85	125	252	161
6	72	92	90	138	261	177
7	83	90	84	100	247	175

Table 9. Average torque generation and power consumption values of the extruder during reprocessing of PP and PP-GNP at 100 rpm and 200 °C.
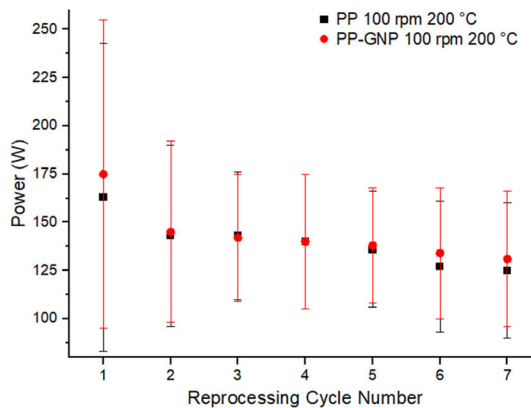
Reprocessing cycle	Average torque generation [Nm]		Average power consumption [W]	
	PP (100 rpm 200 °C)	PP-GNP (100 rpm 200 °C)	PP (100 rpm 200 °C)	PP-GNP (100 rpm 200 °C)
1	83	91	163	175
2	76	77	143	145
3	77	76	143	142
4	72	72	140	140
5	70	72	136	138
6	66	71	127	134
7	64	68	125	131

processing condition B can be attributed to the high torque generation and high screw speed. Compared to LDPE, PS exhibited a more significant decrease in torque and power values as the temperature condition in the extruder increased from 180 to 200 °C. This can be attributed to a substantial drop in the viscosity of PS that may be related to the thermal degradation of PS inside the extruder caused by the greater dependence of viscosity of PS on temperature, compared to LDPE as confirmed by rheological tests reported in the literature.[77] Liu et al.[79] also reported a 38.8% reduction in the apparent viscosity with the shear rate for PS-GNP nanocomposites. Arisawa et al.[81] observed a similar decrease in torque values for PS inside the extruder and discovered that thermal forces could only cause PS deterioration under extreme stress conditions at temperatures of 50 °C. Hence, it is clear that the process control measurements obtained for PS are consistent with previous works.

3.1.3. Process Control Measurements for PP and PP-GNP

The average torque generation and power consumption of the extruder against the number of reprocessing cycles of PP and PP-GNP at 100 rpm and 200 °C (i.e., processing condition A) are shown in **Figure 6** and **Table 9**. During the first cycle,
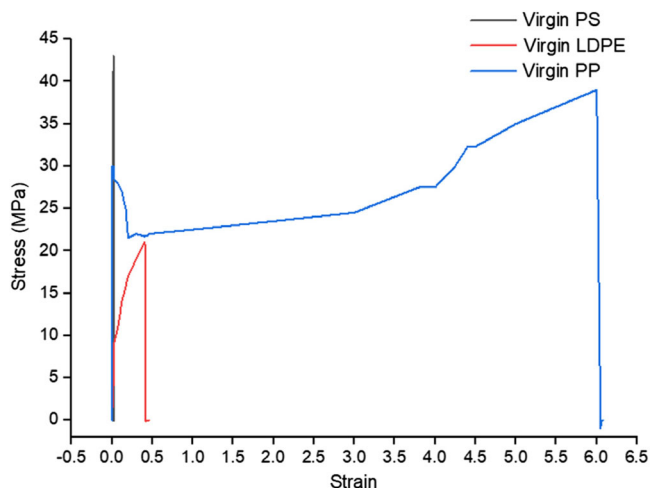
PP-GNP showed higher torque and power values than PP. The incorporation and intercalation of GNP into the polymer are responsible for an increase in the viscosity of the melt at initial reprocessing cycles.[82] According to Triantou et al.[83] reprocessing for several cycles inside an extruder increases the void formation of virgin PP and the crystal phase, while GNP protects the PP matrix from ageing. Processing PP and PP-GNP required similar levels of torque and power from the third cycle to the seventh. The overall decrease in torque with an increasing number of reprocessing cycles suggests that the melt viscosity was decreasing. The decrease in viscosity can be attributed to the reduction in the average molecular weight of the polymer, which indicates that the predominant degradation mechanism was chain scission.[62,84] Botta et al.[85] observed a similar trend of torque values caused by thermal oxidation and degradation inside the extruder.

3.2. Tensile Test Results

3.2.1. Tensile Properties of Virgin Polymers

Figure 7 illustrates the stress–strain curves of virgin LDPE, PS, and PP polymers. The tensile properties of these materials are

Figure 6. Variation of the average torque generation and power consumption of the extruder during reprocessing of PP and PP-GNP at 100 rpm and 200 °C.

Figure 7. Stress–strain curves of virgin polymers.

Table 10. Tensile properties of virgin polymers.

| Polymer	UTS [MPa]	Tensile modulus [MPa]
LDPE	21.3 ± 0.5	211.00 ± 1.3
PS	43.0 ± 0.6	3012.72 ± 2.8
PP	40.0 ± 0.9	1270.00 ± 4.3

shown in **Table 10**. The tensile tests were performed with different strain rates for different materials, as indicated in Table 10. Especially in the case of PS, if the same strain rate as LDPE was used, the samples would have almost failed at a faster rate than the recording frequency itself, resulting in the recording of only a few points.

Figure 7 shows that the yield point of LDPE corresponded to the onset of necking on the physical specimen. The section of the LDPE sample undergoing necking had a smaller cross-section and was therefore subjected to a greater force per unit area, making it more susceptible to deformation, hence the reduction in the gradient of the curve past the yield point. PS did not show the same ductility as LDPE and, in fact, failed in a brittle manner.

The brittle fracture was physically demonstrated by a flat fracture surface on the tensile test specimen, which can be observed by the low strain at break and the absence of a plateau. Polystyrene (PS) typically does not show onset necking during tensile testing due to its brittle nature and lack of significant plastic deformation. Unlike ductile materials that undergo noticeable necking after yielding, PS tends to fail abruptly, showing little or no plastic flow. This brittle behavior is a result of the polymer's molecular structure, where the chains do not easily stretch or slide past each other under stress, leading to immediate fracture rather than necking. Additionally, PS has a low capacity for strain hardening, further contributing to the absence of a necking phase. PP exhibited a ultimate tensile strength (UTS) of 40 MPa and an elongation at break, reaching five times the length of the original specimen length, according to Figure 7. As shown in Table 10, the tensile test results were very close to the standard values obtained from the manufacturers' datasheets, which are displayed in Table 4.

3.2.2. Tensile Properties of Reprocessed LDPE and PS

Figure 8 and **Table 11** illustrate the effect of the screw speed and the temperature condition on the tensile modulus of LDPE and PS over seven reprocessing cycles. It can be observed that the tensile moduli of both LDPE and PS do not exhibit a consistent variation with an increasing number of reprocessing cycles. Freymond et al.[86] reported a random variation in the tensile strength of LDPE up to 11 cycles and concluded that the change in the degree of crystallinity and the size of crystals of LDPE during reprocessing induced fluctuations in the tensile strength. A similar behavior was reported in this study as well due to the variations in the degree of crystallinity and crystal sizes with an increasing number of reprocessing cycles. Hence, the tensile test results did not exhibit an apparent variation with the number of reprocessing cycles. Moreover, the tensile properties of the specimens might also have been affected by defects formed during the injection moulding process. It is expected somewhat that uniaxial tensile test results will be rather inconclusive, as reported in some of the past studies.[87,88] It was reported that impact testing was a technique that reflected the degradation of polymers more vividly. As can be seen from Table 11, PS shows a reduction in the tensile modulus under processing condition 100 rpm 180 °C, compared to the processing condition
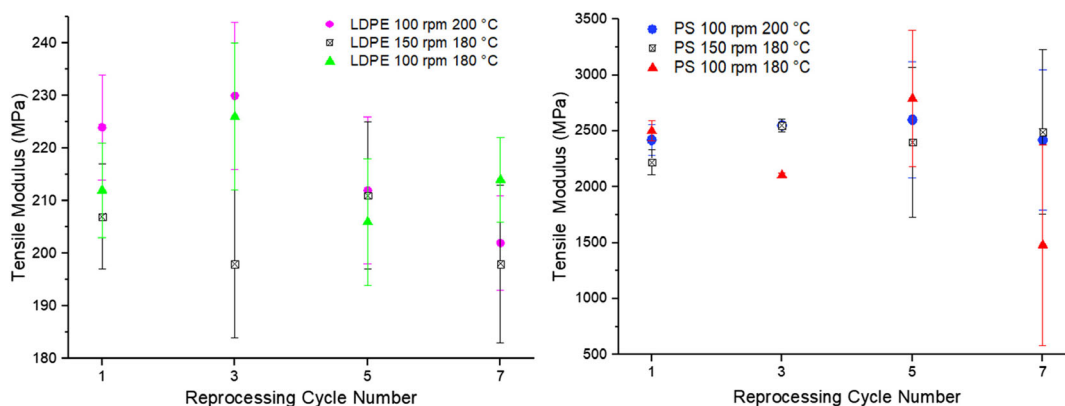
Figure 8. Variation of tensile modulus of LDPE and PS with reprocessing cycles at different processing conditions.

Table 11. Effect of the reprocessing cycle number on the tensile modulus of LDPE and PS.

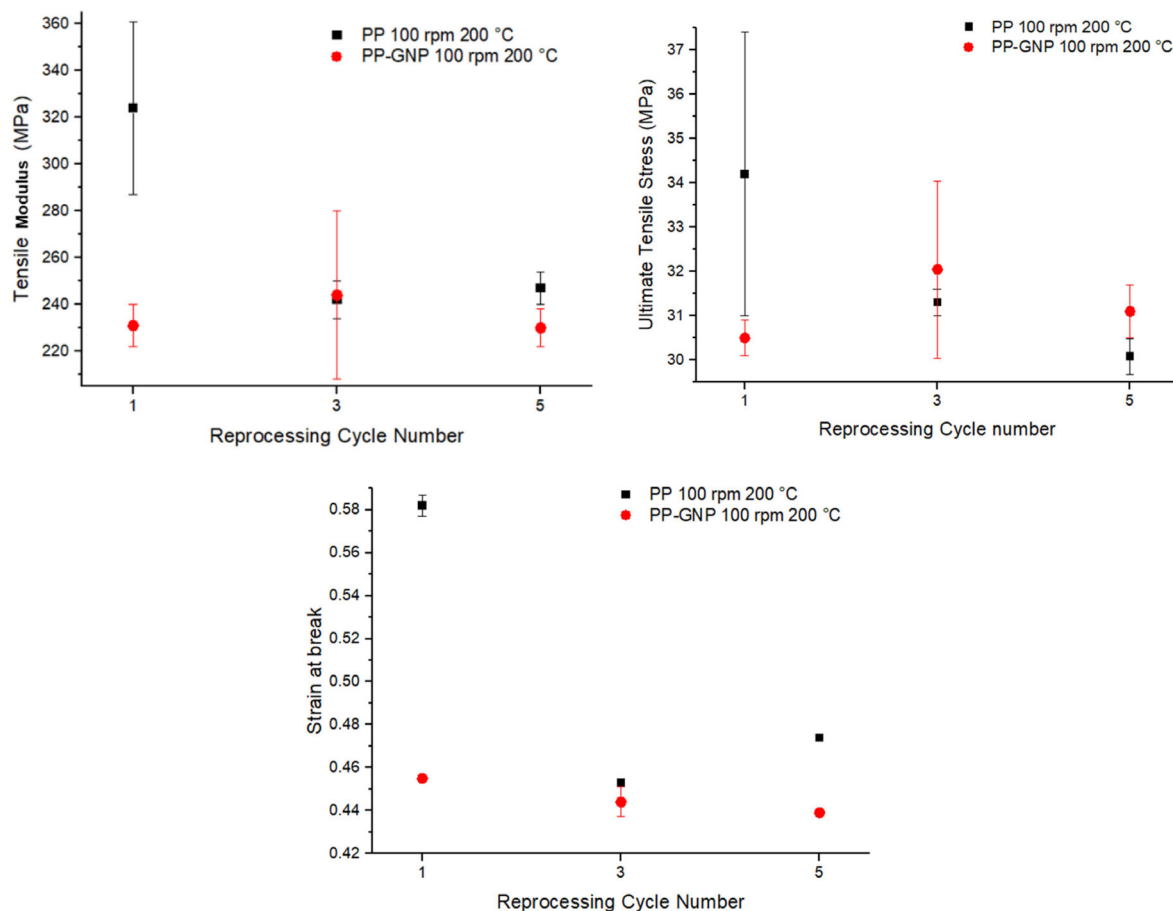| Reprocessing cycle	Average tensile modulus [MPa]					
	LDPE			PS		
	100 rpm 200 °C	150 rpm 180 °C	100 rpm 180 °C	100 rpm 200 °C	150 rpm 180 °C	100 rpm 180 °C
1	224 ± 09	207 ± 10	212 ± 09	2425 ± 177	2223 ± 206	2507 ± 202
3	230 ± 14	198 ± 14	226 ± 12	2550 ± 73	2550 ± 44	2105 ± 48
5	212 ± 16	211 ± 15	206 ± 10	2608 ± 1613	2402 ± 1605	2791 ± 555
7	202 ± 11	198 ± 16	214 ± 07	2423 ± 1286	2494 ± 981	1480 ± 1115

100 rpm 200 °C, after the first and fifth reprocessing cycles. However, an increase in the tensile modulus can be observed after the third and fifth reprocessing cycles at 100 rpm condition for both 180 and 200 °C temperatures. After the seventh cycle, for the both conditions, a drop in tensile modulus was experienced. This could have been caused by the drop in viscosity during reprocessing, where the material was processed at a higher heating condition due to high number of processing cycles and continuous exposure for shear forces. These results also support the previous studies by Saron et al.[89] and Shokoohi et al.[90]

A reduction in the tensile modulus of LDPE can be observed with an increase in the screw speed from 100 to 150 rpm during all reprocessing cycles except for the fifth cycle (see Figure 8). Ding et al.[91] reported a similar behavior in the tensile modulus of LDPE with increasing screw speed caused by macromolecular chain fracture at high processing speeds. Similar results were observed by Shokoohi et al.[90] as well. However, the tensile modulus of PS did not exhibit an apparent variation with increasing screw speed at different reprocessing cycles.

3.2.3. Tensile Properties of Reprocessed PP and PP-GNP

Tensile test results for PP illustrated in **Figure 9** and **Table 12** indicate a significant drop in mechanical performance after

Figure 9. Variation of tensile properties of PP and PP-GNP with reprocessing cycles at 100 rpm and 200 °C.

Table 12. Effect of reprocessing cycles on the tensile properties of PP and PP-GNP at 100 rpm and 200 °C.

Reprocessing cycle	Tensile modulus [MPa]		UTS [MPa]		Strain at break	
	PP	PP-GNP	PP	PP-GNP	PP	PP-GNP
1	324	231	34.2	30.1	0.582	0.455
3	242	244	31.3	32.5	0.453	0.444
5	247	230	30.1	31.1	0.474	0.439

the first reprocessing cycle. The immediate drop in the tensile modulus confirms the prevalence of chain scission during the first extrusion cycle.[83,92] During the processing of the PP homopolymer, radicals are formed by thermomechanical cleavage, consuming traces of oxygen present in the barrel and forming intermediate radical groups containing oxygen.[85] Yang et al.[93] presented a similar type of behavior in glass fiber-reinforced PP composites with a temperature increase from 200 to 240 °C. These radicals are not able to propagate further once the oxygen is consumed and, therefore, terminate by disproportionation, producing $CH_2=C-(CH_3)-$ end groups.[84,94] Also, the thermal oxidation of PP is dominated by intramolecular hydrogen transfer due to the presence of an extra methyl group in the polymer chain. PP undergoes oxidation more readily than PE because the tertiary hydrogen opposite to the methyl group is more prone to oxidation, allowing oxygen to induce chain scission at that site. Oxidation also occurs through free radical chain reaction and is promoted by mechanical stress, heat, and the presence of oxygen and metal catalyst residues[95–97] Consequently, PP degrades preferentially by chain scission. This leads to a drop in the viscosity and the tensile properties with the reduction of molecular weight by degradation. The values of strain at break obtained by this study are presented in **Table 13**. It also resulted in a reduction of yield stress with reprocessing cycles, and the same reasoning for the drop in tensile strength observed was attributed to degradation caused by chain scission and thermal oxidation.

PP-GNP composites exhibited a slight rise in the tensile modulus and the UTS from the first cycle to the third and then a reduction from the third cycle to the fifth. The reduction in the tensile modulus was for similar reasons as for PP. The interfacial interactions between GNP and PP worsened due to PP chain deformation with thermal degradation and oxidation processes. GNP acted as a foreign material to the polymer matrix and anticipated initial crack propagation. This has resulted in

Table 13. Mechanical properties of PP after 0, 1, 3, and 5 extrusion cycles at 260 °C, reported in the study by Tocháček et al. (2008).

Property	Extrusion cycle			
	Before extrusion	1st extrusion cycle	3rd extrusion cycle	5th extrusion cycle
Stress at yield [MPa]	29.9 ± 0.1	29.5 ± 0.1	29.4 ± 0.1	29.2 ± 0.1
Elongation at break [%]	67.3 ± 23	54.8 ± 16	59.1 ± 4.2	56.3 ± 18

PP-GNP having a lower stiffness than PP. Ahmad et al.[98] reported a similar behavior in GNP reinforced PP with a GNP loading of 5 wt%, and the tensile modulus of the composite was reduced by 5 MPa from 0 to 5 wt% GNP. However, the rise in the tensile modulus of PP-GNP by 13 MPa after the first cycle was due to the uniform dispersion of GNP and crosslink formation in the PP matrix, as shown in **Figure 10**. A similar finding has been reported by Al-Saleh et al.[92] experiencing a growth in the tensile strength from 16.5 to 20.18 MPa with an increase from 0 to 5 wt% of GNP loading, while El Achaby et al.[99] reported a 27.59 MPa increase in the tensile strength with GNP loading varying from 0 to 3 wt% in PP-GNP nanocomposites, and both studies concluded the same reason for this behavior. As evident from Table 12, the UTS values of PP-GNP after the third and fifth reprocessing cycles were found to be greater than those of PP. This is obvious as the crosslink formation and reinforcement of PP-GNP are higher than those of PP due to the continuous mixing of GNP inside the PP matrix with an increasing number of reprocessing cycles.

3.3. Differential Scanning Calorimetry Results

Figure 11 illustrates the DSC curves for PS samples from different reprocessing cycles under different processing conditions, and there is no identification of a clear melting peak. A peak between 90 and 100 °C could be identified, which is related to polymer bead collapsing. The findings of Maafa et al.[100] also support the results observed here. The virgin PS curve corresponds to DSC for PS and it degrades thermally at higher temperatures due to exposure to greater heat, hence the molecular weight is reduced considerably. Akintola et al.[101] reported similar results in their study on functional polymer-based composites. There was only a "kink" in the curve below 100 °C, showing what could be the glass transition temperature (T_g). A consistent trend in the shift of the DSC curves was also not identified. The DSC curves of all reprocessed PS samples exhibit higher heat flow values compared to virgin PS due to thermal degradation occurring during reprocessing. This degradation leads to chain scission, reducing the molecular weight and altering the polymer's thermal behavior. Consequently, less energy is required to induce phase transitions, resulting in higher heat flow values.[102]

Figure 12 illustrates the DSC curves of LDPE reprocessed at different processing conditions. The curve for virgin LDPE displays all its characteristic thermal properties. The section of the curve where the line dips into the trough indicates the onset temperature, and as expected, this is found to be around 100 °C. Rosa et al.[103] and Poh et al.[104] reported results similar to the value obtained. The curve has a negative gradient ahead of the melting point trough because of the semicrystalline nature of this polymer.[105] The broader size distribution of crystallites causes them to start melting at a wider range of temperatures.[106] The successive reprocessing cycles shifted the curve upwards for LDPE, reducing the area enclosed by the DSC curve. This corresponded to a decrease in the enthalpy of fusion of the polymer and, therefore, a reduction in the crystallinity.[107] It can be deduced that reprocessing caused partial destruction of crystalline domains with an increase in the number of reprocessing
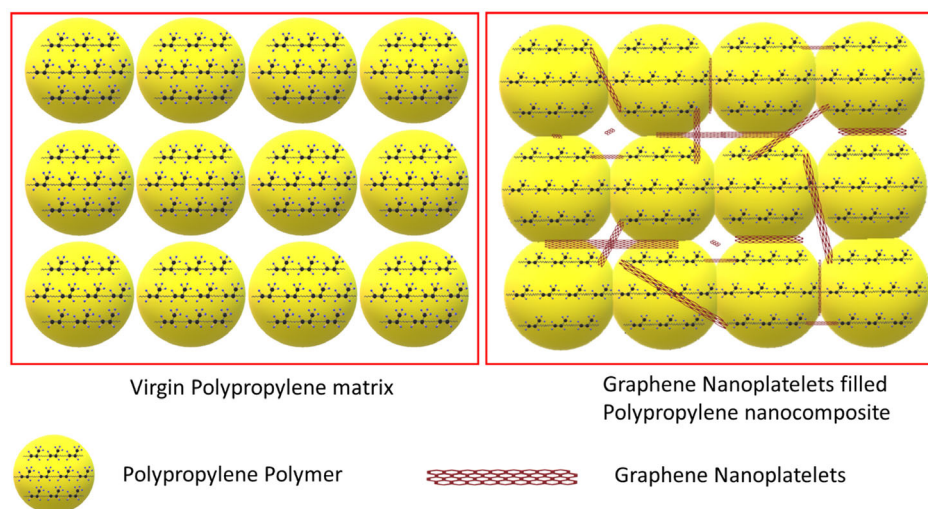
**ADVANCED
SCIENCE NEWS**

www.advancedsciencenews.com

**ADVANCED
ENGINEERING
MATERIALS**

www.aem-journal.com

Figure 10. A schematic showing the possible crosslink formation between GNP and PP.

Figure 11. DSC curves of virgin and reprocessed PS at different processing conditions.
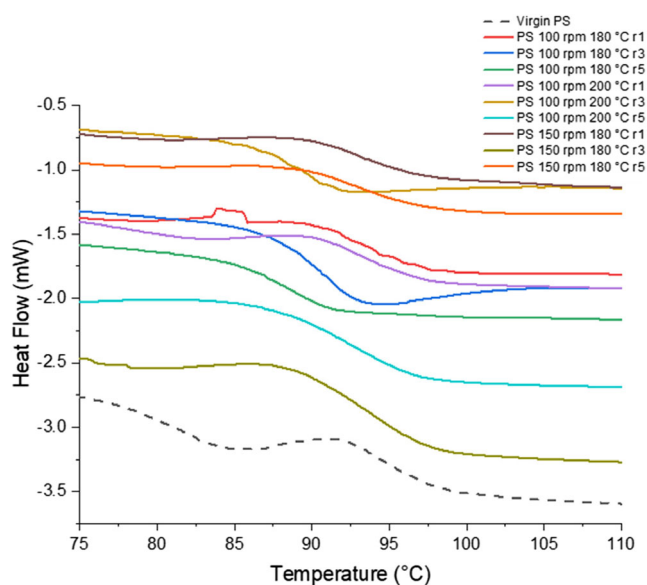

Figure 12. DSC curves of virgin and reprocessed LDPE at different processing conditions.

cycles.[108] Due to the changes in crystallinity, an apparent variation of the melting point of LDPE under the three processing conditions could not be observed (see **Figure 13** and **Table 14**). However, the melting point of LDPE samples after the first cycle showed similar findings as reported by Ding et al.[91] who observed a diminishing trend in the fusion enthalpy (about 3 Jg^{-1}) with an increase in the screw speed from 50 to 150 rpm. The same phenomenon was not observed in PS, where the evolution of the DSC curves does not show a clear shift, as shown in Figure 11. Reasonably, PS could not have been subjected to a reduction in crystalline domains due to its amorphous nature.

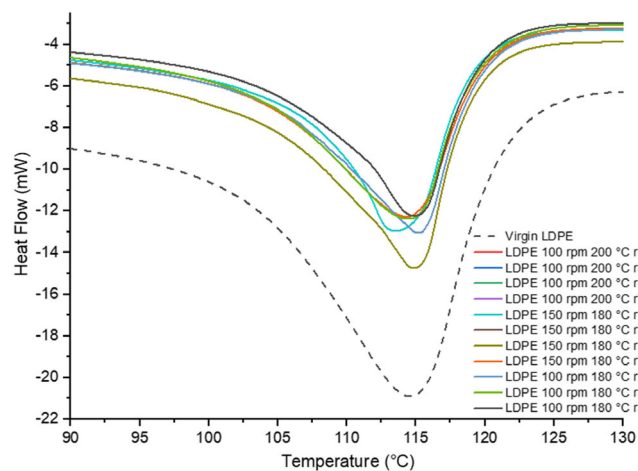**Figure 14** illustrates the DSC curves of the reprocessed PP and PP-GNP materials. **Figure 15** and **Table 15** present the variation of the melting points of PP and PP-GNP with increasing reprocessing cycles. The melting point of both materials increased with an increasing number of reprocessing cycles up to the fifth cycle. It can be observed that PP has a higher melting point than PP-GNP after the initial reprocessing cycles. Al-Saleh et al.[92] reported a similar behavior of the melting point due to a weak nucleation effect of GNP on PP. However, GNPs function as a nucleating agent, causing the alpha (α) crystalline phase of PP to develop epitaxially. The particle surface that is open to heterogeneous nucleation has an impact on the nucleating effect.[109] It is noticed that the tiniest micrometric particles exhibit radial spherulitic growths. Because they are easily orientated by flow, the coarsest GNPs promote the trans crystallinity of PP, causing the (010) plane of PP to align with the (001) plane of graphene nanoplatelets.[110] Ajorloo et al.[111] reported an opposite behavior, where the melting point of PP-GNP was found to be 14 °C higher than the melting point of PP, owing to the β-crystal formation at 3 (vol%) GNP loading. The findings by
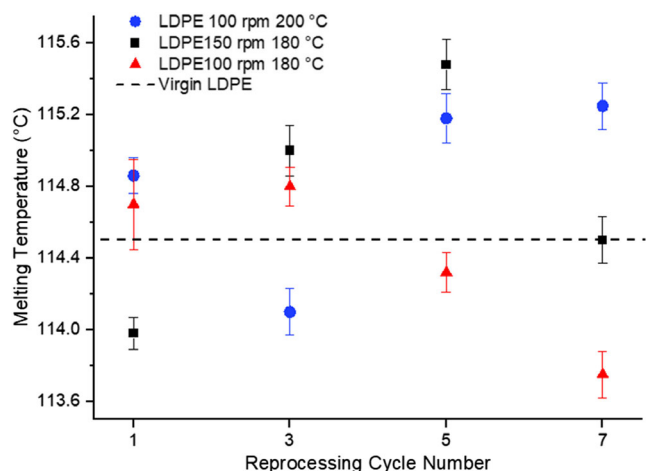
Figure 13. Variation of the melting temperature of LDPE with reprocessing cycles at different processing conditions.

Table 14. Effect of reprocessing cycles on the melting temperature of LDPE.

Reprocessing cycle	Melting temperature [°C]		
	100 rpm 200 °C	150 rpm 180 °C	100 rpm 180 °C
1	114.8	113.9	114.7
3	114.1	115.0	114.8
5	115.2	115.4	114.3
7	115.3	114.5	113.8
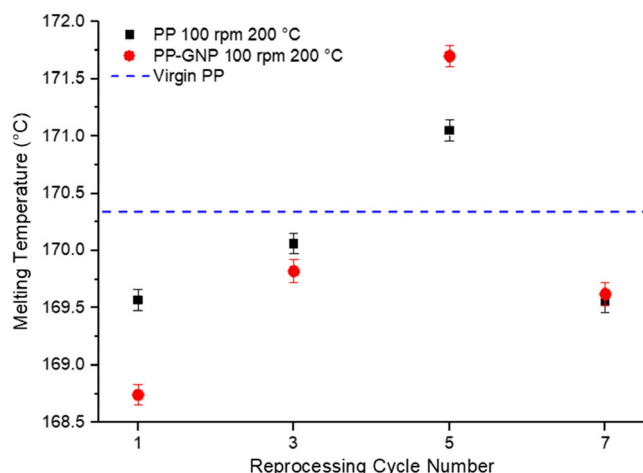
Figure 15. Variation of the melting temperature of PP and PP-GNP with reprocessing cycles.

Table 15. Effect of reprocessing cycles on the melting temperature of PP and PP-GNP.

Reprocessing cycle	Melting temperature [°C]	
	PP (100 rpm 200 °C)	PP-GNP (100 rpm 200 °C)
1	169.57	168.74
3	170.06	169.82
5	171.05	171.7
7	169.55	169.62
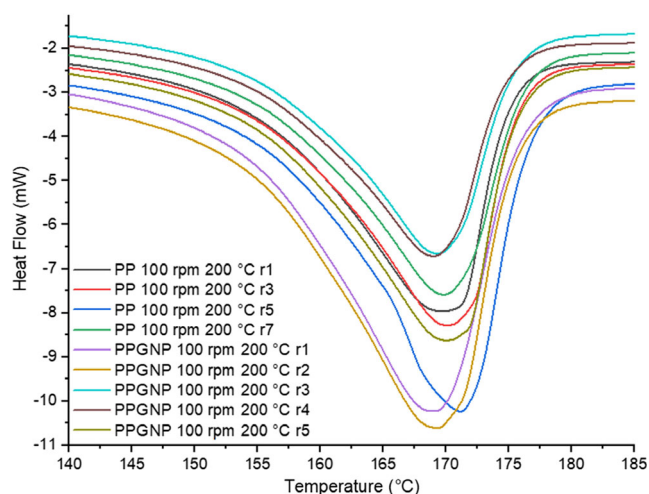
Figure 14. DSC curves of reprocessed PP and PP-GNP.

Abdou et al.[112] and Kalaitzidou et al.[113] based on DSC results of PP and PP-GNP composites also support these results. Ajorloo et al.[111] further observed a higher melting point of the composite with a reduction in the particle size of GNP and a lower melting point at higher GNP loading for branched PP. As shown in Figure 15, the melting points of both polymer

and polymer composite have increased from the first cycle to the fifth and diminished from the fifth cycle to the seventh. The DSC results are in conflict with the tensile test results, which exhibited an apparent molecular weight reduction effect in PP-GNP. Here, an increase in melting temperature would correlate to a more likely occurrence of chain crosslinking, as shown in Figure 10.[92] Thermal degradation with the heat generated inside the extruder reduces the melting point after the fifth reprocessing cycle.[114]

3.4. Key Findings of the Study

According to the results reported in Section 3.1–3.3, the key findings of this study can be summarized as presented in **Table 16**.

4. Tackling Polymeric Waste and Sustainable Development Goals

The United Nations Sustainability Goals, also known as the Sustainable Development Goals (SDGs), encompass a comprehensive set of 17 global objectives designed to tackle pressing social, economic, and environmental challenges by the year 2030.[115] Among these goals, environmental sustainability holds paramount importance, and one notable avenue for achieving this is through the recycling and reuse of polymers, as plastic-based waste has been a global disaster and can be found all over

Table 16. Key findings based on the results of the study.

Parameter/Property	Material	Processing condition	Key findings
Torque and power	LDPE	Screw speed (from 100–150 rpm)	Increase in torque and power with increasing screw speed at all reprocessing cycles.
		Set temperature (from 180–200 °C)	No significant effect on torque and power.
	PS	Screw speed (from 100–150 rpm)	Increase in power with increasing screw speed at all reprocessing cycles.
		Set temperature (from 180–200 °C)	Decrease in torque and power with increasing set temperatures at all reprocessing cycles.
	PP and PP-GNP	100 rpm screw speed at 200 °C set temperature	Torque and power decreased with an increasing number of reprocessing cycles. A higher torque and power consumption were observed with PP-GNP compared to PP during the first reprocessing cycle.
Tensile properties	LDPE	Screw speed (from 100–150 rpm)	Tensile modulus decreased with increasing screw speed except at the fifth reprocessing cycle.
		Set temperature (from 180–200 °C)	Tensile modulus increased with increasing set temperatures except at the seventh reprocessing cycle. A general reduction in tensile modulus was observed with an increasing number of reprocessing cycles at the 200 °C temperature condition. However, no significant effect on the tensile modulus was observed with an increasing number of reprocessing cycles at other processing conditions.
	PS	Screw speed (from 100–150 rpm)	Tensile modulus decreased with increasing screw speed at the first and fifth reprocessing cycles and increased at the third and seventh reprocessing cycles. No consistent variation in the tensile modulus was observed with an increasing number of reprocessing cycles.
		Set temperature (from 180–200 °C)	Tensile modulus decreased with increasing set temperatures at the first and fifth reprocessing cycles and increased at the third and seventh reprocessing cycles. No consistent variation in the tensile modulus was observed with an increasing number of reprocessing cycles.
	PP	100 rpm screw speed at 200 °C set temperature	A significant reduction in tensile properties was observed after the first reprocessing cycle.
	PP-GNP		Tensile strength and modulus increased at the third reprocessing cycle and then reduced at the fifth reprocessing cycle. Strain at break is reduced with an increasing number of reprocessing cycles. Tensile properties of PP-GNP showed a significant reduction compared to PP after the first reprocessing cycle.
Thermal properties	LDPE	Screw speed (from 100–150 rpm) Set temperature (from 180–200 °C)	No clear variation in the melting point was observed with increasing screw speed, increasing set temperatures, or increasing number of reprocessing cycles.
	PS	Screw speed (from 100–150 rpm) Set temperature (from 180–200 °C)	A peak at 90–100 °C could be identified in the DSC curve caused by the polymer bead collapsing.
	PP and PP-GNP	100 rpm screw speed at 200 °C set temperature	The melting point increased with an increasing number of reprocessing cycles up to the fifth cycle and decreased after the seventh cycle.

the world in waters, lands, and air. **Figure 16**a shows an image of part of the great Pacific garbage patch, which is part of the five offshore plastic accumulation zones (see Figure 16b) in the oceans, and this is located between Hawaii and California. It has been estimated that this covers a surface area of 1.6 million square kilometers, and, for example, this is an area equivalent to twice the size of Texas and three times the size of France. Moreover, it has been estimated that between 1.15 and 2.41 million tons of plastics are entering the ocean annually, mainly via rivers[116]

Under these tragic circumstances, recycling plastic waste has become a global priority. The process of recycling and reusing polymers has emerged as a vital contributor to environmental sustainability. It has yielded significant results in various areas: firstly, recycling and reusing polymers make a substantial impact in reducing resource consumption. Reprocessing LDPE, PP, and PS polymers has a profound impact on the United Nations Sustainability Goals as they are among the most commonly used polymers in the world at present. Recycling initiatives instead of landfilling and incineration of plastic waste can reduce demand for virgin materials such as petroleum-based feedstocks, which directly contributes to Goal 12: Responsible Consumption and Production. By reprocessing these polymers, responsible consumption patterns can be promoted by extending their lifecycle
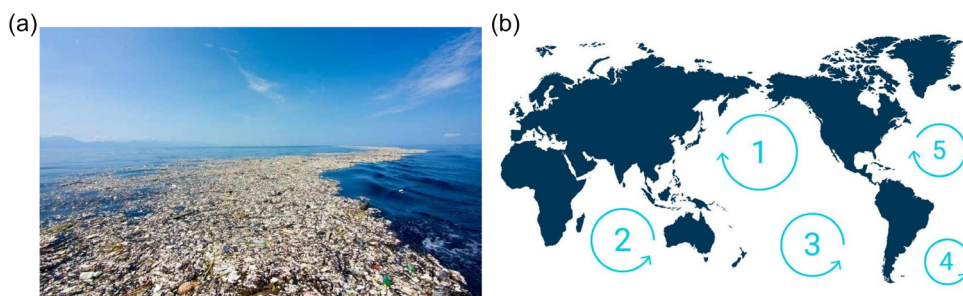
Figure 16. a) An image showing part of the great Pacific garbage patch, b) an illustrative map showing the five major offshore plastic accumulation zones worldwide. Reproduced with permission.[116] Copyright 2019, Forbes.

and reducing the demand for new plastic production. This helps in achieving sustainable resource management and reducing the environmental footprint associated with plastic consumption.[97]

Moreover, recycling and reusing of polymers play a crucial role in waste reduction and pollution prevention. PP, LDPE, and PS, when discarded, can persist in the environment for extended periods, polluting ecosystems. By engaging in polymer recycling, indeed, it is possible to prevent plastic waste from accumulating in landfills or finding its way into our oceans, thus supporting Goal 14: Life Below Water and Goal 15: Life on Land. By diverting these polymers from landfills and incineration, the pollution risks they pose to marine and terrestrial ecosystems are mitigated. Reprocessing minimizes plastic waste accumulation and ensures that these materials are given a second life, significantly reducing environmental pollution and safeguarding delicate ecosystems.[115] This process further caters to achieving Goal 11: Sustainable Cities and Communities. Proper management of polymer waste can contribute to creating clean and sustainable cities through recycling and reusing polymers and reducing the volume of waste sent to landfills. In addition, recycling and reusing polymers contribute to energy conservation and the reduction of greenhouse gas emissions. The energy required to recycle plastics is considerably lower than that needed to manufacture virgin materials.[117] This energy efficiency aligns with Goal 7: Affordable and Clean Energy. Furthermore, recycling contributes to the reduction of greenhouse gas emissions, supporting Goal 13: Climate Action. Reprocessing polymers helps mitigate the carbon footprint and combat climate change by reducing the environmental impact of plastic production. Furthermore, the concept of recycling and reusing polymers promotes the adoption of a circular economy. Hence, the reprocessing of polymers promotes a circular economy, aligning with Goal 9: Industry, Innovation, and Infrastructure. By collecting, sorting, and reprocessing these materials, it is possible to establish a closed-loop system that allows for repeated reuse. This reduces the dependence on new plastic production, encourages sustainable industrial practices, and fosters innovation in recycling technologies.

Apart from the environmental pillar, recycling, and reusing polymers also contribute to the socio-economic bottom lines as well. Encouraging the development of innovative recycling technologies and infrastructure can enhance the efficiency and effectiveness of polymer recycling, which drives technological advancements and promotes sustainable industrial practices

by aligning with Goal 9: Industry, Innovation, and Infrastructure. This practice can further be extended to attain Goal 8: Decent Work and Economic Growth. Expanding the polymer recycling and reuse industry creates job opportunities and fosters economic growth. Finally, the process of recycling and reusing polymers would directly cater toward achieving SDG 1: No Poverty and indirectly toward SDG 2: Zero Hunger, as well.[115]

Through concerted efforts in recycling and reusing polymers, significant strides have been made toward achieving various UN Sustainability Goals. These efforts exemplify responsible consumption, environmental protection, sustainable production, decent work and economic growth, and no poverty, and all of these should help to propel us closer to a more sustainable and inclusive future.[118,119] In summary, reprocessing polymers/plastics/ or related composites significantly contributes to multiple United Nations Sustainability Goals. Likewise, it promotes responsible consumption, reduces waste and pollution, combats climate change, and drives the transition toward a circular economy. Eventually, this will shed light on achieving a more sustainable and inclusive future for our planet.

5. Conclusions

This study was conducted to examine the effect of processing conditions and the number of reprocessing cycles on the mechanical and thermal properties of LDPE, PS, PP, and (1 % w/w) GNP-reinforced PP nanocomposite materials. The process of thermomechanical recycling was simulated on a smaller scale by reprocessing the materials up to seven extrusion cycles under three different processing conditions on a twin-screw extruder. The experiments did not account for the level of impurities usually present in polymer waste streams.

An increase in the torque and power consumption was observed for LDPE and PS with increasing screw speed due to the high shear forces at high screw speeds. However, the torque and power consumption decreased with increasing set temperatures for PS due to chain scission and thermal degradation. GNP disturbed the void formation of PP and protected PP from chain scission through the reinforcement between polar groups. Therefore, PP-GNP consumed more power compared to PP during the first reprocessing cycle. The tensile properties of LDPE and PS were found to have been affected by the processing conditions (i.e., screw speed and set temperatures).

However, no consistent variation in the tensile properties was observed with an increasing number of reprocessing cycles for both LDPE and PS. The tensile properties of PP were found to have reduced significantly after the first reprocessing cycle, while the tensile properties of PP-GNP exhibited a significant reduction compared to PP after the first reprocessing cycle. In terms of thermal properties, the melting point of LDPE did not report a clear variation with the processing conditions and the number of reprocessing cycles. A peak at 90–100 °C was identified in the DSC curve of PS, which was attributed to polymer bead collapsing. The melting points of PP and PP-GNP increased with an increasing number of reprocessing cycles up to five cycles and then decreased after the seventh cycle.

In future work, direct measurements of average molecular weight, as well as flexural and impact testing on both virgin and GNP-filled composites, could be conducted to gain more detailed insights into the material properties and performance. Scanning electron microscopic images of cross-sections of fractured tensile specimens would be beneficial to examine the fracture surfaces to understand the fracture behavior. Comparative studies on waste polymers with various types of fillers should be implemented further to achieve better properties of reprocessed polymers. In the processing conditions, by altering screw rotational speed and temperature during reprocessing cycles, the number of cycles for optimum properties could be detected. Also, by changing the filler loading in polymer nanocomposites, property variations could be investigated further. Moreover, polymer blending would be beneficial to improve the properties of the matrix and by varying the percentage of each polymer inside the blends and composites, properties could be tested in different reprocessing conditions.

Conflict of Interest

The authors declare no conflict of interest.

Data Availability Statement

The data that support the findings of this study are available from the corresponding author upon reasonable request.

[1] C. Abeykoon, A. L. Kelly, J. Vera-Sorroche, E. C. Brown, P. D. Coates, J. Deng, K. Li, E. Harkin-Jones, M. Price, *Appl. Energy* **2014**, *135*, 560.

[2] V. Dananjaya, S. Marimuthu, R. (Chunhui) Yang, A. N. Grace, C. Abeykoon, *Prog. Mater. Sci.* **2024**, *144*, 101282.

[3] S. A. V. Dananjaya, U. M. S. Priyanka, Y. R. Somarathna, L. Karunanayake, S. Siriwardena, *J. Vinyl Addit. Technol.* **2022**, *28*, 907.

[4] S. A. V. Dananjaya, Y. R. Somarathna, L. Karunanayake, S. Siriwardena, *J. Rubber Res. Inst. Sri Lanka* **2022**, *102*, 1.

[5] S. A. V. Dananjaya, Y. R. Somarathna, L. Karunanayake, S. Siriwardena, *J. Polym. Res.* **2022**, *29*, 71.

[6] A. Elbazze, B. Radi, *Int. Rev. Mech. Eng.* **2022**, *16*, 249.

[7] V. Dananjaya, Y. Somarathna, S. Siriwardena, N. Sirimuthu, L. Karunanayake, C. Abeykoon, *Int. J. Lightweight Mater. Manuf.* **2024**, *7*, 450.

[8] S. A. V. Dananjaya, V. S. Chevali, J. P. Dear, P. Potluri, C. Abeykoon, *Prog. Mater. Sci.* **2024**, *146*, 101336.

[9] M. R. Johansen, T. B. Christensen, T. M. Ramos, K. Syberg, *J. Environ. Manag.* **2022**, *302*, 113975.

[10] K. P. Pramoda, H. Hussain, H. M. Koh, H. R. Tan, C. B. He, *J. Polym. Sci. A: Polym. Chem.* **2010**, *48*, 4262.

[11] X. Sun, P. Ramesh, M. E. Itkis, E. Bekyarova, R. C. Haddon, *J. Phys. Condens. Matter* **2010**, *22*, 334216.

[12] L. Hu, T. Desai, P. Keblinski, *J. Appl. Phys.* **2011**, *110*, 033517.

[13] M. Shtein, R. Nadiv, M. Buzaglo, K. Kahil, O. Regev, *Chem. Mater.* **2015**, *27*, 2100.

[14] R. J. Young, M. Liu, I. A. Kinloch, S. Li, X. Zhao, C. Vallés, D. G. Papageorgiou, *Compos. Sci. Technol.* **2018**, *154*, 110.

[15] S. Vadukumpully, J. Paul, N. Mahanta, S. Valiyaveettil, *Carbon* **2011**, *49*, 198.

[16] E. Lago, P. S. Toth, G. Pugliese, V. Pellegrini, F. Bonaccorso, *RSC Adv.* **2016**, *6*, 97931.

[17] P. Zapata, R. Quijada, E. Retuer, E. Moncada, *J. Chil. Chem. Soc.* **2008**, *53*, https://www.scielo.cl/scielo.php?script=sci_arttext&pid=S0717-97072008000100006.

[18] L. Mrah, R. Meghabar, *Polym. Bull.* **2021**, *78*, 3509.

[19] H.-W. Kim, C. W. Macosko, *Polymer* **2009**, *50*, 3797.

[20] H. Bin Zhang, W. G. Zheng, Q. Yan, Y. Yang, J. W. Wang, Z. H. Lu, G. Y. Ji, Z. Z. Yu, *Polymer* **2010**, *51*, 1191.

[21] W. P. Wang, Y. Liu, X. X. Li, Y. Z. You, *J. Appl. Polym. Sci.* **2006**, *100*, 1427.

[22] M. Mokhtari, E. Archer, N. Bloomfield, E. Harkin-Jones, A. McIlhagger, *Polym. Int.* **2021**, *70*, 1137.

[23] S. J. Lee, S. J. Yoon, I. Y. Jeon, *Polymers* **2022**, *14*, 4733.

[24] H. V. Madhad, D. V. Vasava, *J. Thermoplast. Composite Mater.* **2022**, *35*, 570.

[25] C. M. Rochman, M. A. Browne, A. J. Underwood, J. A. Van Franeker, R. C. Thompson, L. A. Amaral-Zettler, *Ecology* **2016**, *97*, 302.

[26] E. E. Burns, A. B. A. Boxall, *Environ. Toxicol. Chem.* **2018**, *37*, 2776.

[27] R. Geyer, J. R. Jambeck, K. L. Law, *Sci. Adv.* **2017**, *3*, e1700782.

[28] L. Ribba, M. Lopretti, G. Montes De Oca-Vásquez, D. Batista, S. Goyanes, J. R. Vega-Baudrit, *Environ. Res. Lett.* **2022**, *17*, 033003.

[29] J. D. Chea, K. M. Yenkie, J. F. Stanzione, G. J. Ruiz-Mercado, *J. Hazard. Mater.* **2023**, *441*, 129902.

[30] David C. Wilson, *Global Waste Management Outlook 2015*, UNEP, Nairobi **2015**.

[31] W. W. Y. Lau, Y. Shiran, R. M. Bailey, E. Cook, M. R. Stuchtey, J. Koskella, C. A. Velis, L. Godfrey, J. Boucher, M. B. Murphy, R. C. Thompson, E. Jankowska, A. C. Castillo, T. D. Pilditch, B. Dixon, L. Koerselman, E. Kosior, E. Favoino, J. Gutberlet, S. Baulch, M. E. Atreya, D. Fischer, K. K. He, M. M. Petit, U. R. Sumaila, E. Neil, M. V. Bernhofen, K. Lawrence, J. E. Palardy, *Science* **2020**, *369*, 1455.

[32] C. A. Velis, B. D. Hardesty, J. W. Cottom, C. Wilcox, *Environ. Sci. Policy* **2022**, *138*, 20.

[33] P. Garcia-Gutierrez, A. M. Amadei, D. Klenert, S. Nessi, D. Tonini, D. Tosches, F. Ardente, H. Saveyn, *Environmental and Economic Assessment of Plastic Waste Recycling*, Publications Office of the European Union, Luxembourg **2023**, https://publications.jrc.ec.europa.eu/repository/handle/JRC132067.

[34] U. Arena, F. Ardolino, *Resour. Conserv. Recycl.* **2022**, *183*, 106379.

[35] *Global Material Resources Outlook to 2060*, OECD **2019**, https://www.oecd.org/en/publications/global-material-resources-outlook-to-2060_9789264307452-en.html.

[36] S. Khadke, P. Gupta, S. Rachakunta, C. Mahata, S. Dawn, M. Sharma, D. Verma, A. Pradhan, A. M. S. Krishna, S. Ramakrishna, S. Chakrabortty, G. Saianand, P. Sonar, S. Biring, J. K. Dash, G. K. Dalapati, *Sustainability* **2021**, *13*, 9142.

[37] J. Hopewell, R. Dvorak, E. Kosior, *Philos. Trans. R Soc. B: Biol. Sci.* **2009**, *364*, 2115.

[38] A. Kijo-Kleczkowska, A. Gnatowski, *Energies* **2022**, *15*, 2114.

[39] J. Aguado, J. Carlos, D. Serrano, *Glob. NEST J.* **2018**, *9*, 12.

[40] C. I. Idumah, I. C. Nwuzor, *SN Appl. Sci.* **2019**, *1*, 1402.

[41] I. Wojnowska-Baryła, K. Bernat, M. Zaborowska, *Int. J. Environ. Res. Public Health* **2022**, *19*, 13223.

[42] N. Bahlouli, D. Pessey, C. Raveyre, J. Guillet, S. Ahzi, A. Dahoun, J. M. Hiver, *Mater. Des.* **2012**, *33*, 451.

[43] D. Jubinville, E. Esmizadeh, C. Tzoganakis, T. Mekonnen, *Composites, B* **2021**, *219*, 108873.

[44] M. Tanahashi, *Materials* **2010**, *3*, 1593.

[45] E. Hammel, X. Tang, M. Trampert, T. Schmitt, K. Mauthner, A. Eder, P. Pötschke, *Carbon* **2004**, *42*, 1153.

[46] P. N. Khanam, M. Almaadeed, S. Almaadeed, S. Kunhoth, M. Ouederni, D. Sun, A. Hamilton, E. H. Jones, B. Mayoral, *Int. J. Polym. Sci.* **2016**, *2016*, 1.

[47] C. Abeykoon, *Polymer Extrusion: A Study on Thermal Monitoring Techniques and Melting Issues*, Lap Lambert Academic Publishing **2012**, https://www.researchgate.net/publication/259687188_Polymer_Extrusion_A_Study_on_Thermal_Monitoring_Techniques_and_Melting_Issues.

[48] H. Garcia-Vazquez, M. Trujillo-Barragán, M. Rodriguez-Juarez, E. Mondragon-Flores, B. Millan-Malo, J. Villada, M. E. Rodriguez-García, *Effect of the Thermomechanical Reprocessing Conditions on Polypropylene Composites Based Automotive Waste Parts*, **2022**, https://papers.ssrn.com/sol3/papers.cfm?abstract_id=4121971.

[49] C. Abeykoon, *Modelling and Control of Melt Temperature in Polymer Extrusion*, **2011**, https://www.researchgate.net/publication/259687063_Modelling_and_Control_of_Melt_Temperature_in_Polymer_Extrusion.

[50] C. Abeykoon, P. J. Martin, K. Li, A. L. Kelly, *Appl. Math. Model* **2014**, *38*, 1224.

[51] C. Abeykoon, K. Li, M. McAfee, P. J. Martin, J. Deng, A. L. Kelly, *Modelling the Effects of Operating Conditions on Die Melt Temperature Homogeneity in Single Screw Extrusion*, **2010**, https://www.researchgate.net/publication/259686961_Modelling_the_Effects_of_Operating_Conditions_on_Die_Melt_Temperature_Homogeneity_in_Single_Screw_Extrusion.

[52] C. Abeykoon, P. Pérez, A. L. Kelly, *Polym. Eng. Sci.* **2020**, *60*, 1244.

[53] J. Gálvez, J. P. Correa Aguirre, M. A. Hidalgo Salazar, B. V. Mondragón, E. Wagner, C. Caicedo, *Polymers* **2020**, *12*, 2111.

[54] P. G. Lafleur, B. Vergnes, *Polymer Extrusion*, Hanser Publishers, Munich **2014**.

[55] O. Agboola, R. Sadiku, T. Mokrani, I. Amer, O. Imoru, *Polyolefin Fibres: Structure, Properties And Industrial Applications: Second Edition*, Woodhead Publishing Ltd, Darya Ganj **2017**, p. 89.

[56] J. Drabek, M. Zatloukal, *Polymers* **2016**, *8*, 317.

[57] S. Venkatachalam, Shilpa G., Jayprakash V., Prashant R., Krishna Rao, Anil K., in *Polyester* (Ed: H.E.-D.M. Saleh), InTech, Rijeka **2012**, Ch. 4.

[58] Z. Gao, T. Kaneko, I. Amasaki, M. Nakada, *Polym. Degrad. Stab.* **2003**, *80*, 269.

[59] G. Scott, *Polym. Degrad. Stab.* **1995**, *48*, 315.

[60] H. Jin, J. Gonzalez-Gutierrez, P. Oblak, B. Zupančič, I. Emri, *Polym. Degrad. Stab.* **2012**, *97*, 2262.

[61] M. J. Abad, A. Ares, L. Barral, J. Cano, F. J. Díez, S. García-Garabal, J. López, C. Ramírez, *J. Appl. Polym. Sci.* **2004**, *92*, 3910.

[62] J. Aurrekoetxea, M. A. Sarrionandia, I. Urrutibeascoa, M. L. Maspoch, *J. Mater. Sci.* **2001**, *36*, 2607.

[63] P. W. Huang, H. S. Peng, *Sustainability* **2021**, *13*, 11085.

[64] L. Incarnato, P. Scarfato, D. Acierno, *Polym. Eng. Sci.* **1999**, *39*, 749.

[65] C. Aumnate, N. Rudolph, M. Sarmadi, *Polymers* **2019**, *11*, 1456.

[66] N. Rust, E. E. Ferg, I. Masalova, *Polym. Test.* **2006**, *25*, 130.

[67] E. Fuenmayor, M. Forde, A. V. Healy, D. M. Devine, J. G. Lyons, C. McConville, I. Major, *Pharmaceutics* **2018**, *10*, 44.

[68] Y. Lin, T. B. Kouznetsova, C. C. Chang, S. L. Craig, *Nat. Commun.* **2020**, *11*, 4987.

[69] M. Alotaibi, T. Aldhafeeri, C. Barry, *Polymers* **2022**, *14*, 2661.

[70] P. N. Khanam, M. Almaadeed, S. Almaadeed, S. Kunhoth, M. Ouederni, D. Sun, A. Hamilton, E. H. Jones, B. Mayoral, *Int. J. Polym. Sci.* **2016**, *2016*, https://doi.org/10.1155/2016/5340252.

[71] K. Ono, M. Yamaguchi, *J. Appl. Polym. Sci.* **2009**, *113*, 1462.

[72] F. Castéran, K. Delage, N. Hascoët, A. Ammar, F. Chinesta, P. Cassagnau, *Polymers* **2022**, *14*, 800.

[73] Y. Teymouri, *Int. J. Mater. Sci. Appl.* **2014**, *3*, 168.

[74] S. J. Zack, N. T. Herrold, K. Wakabayashi, *SPE Polym.* **2022**, *3*, 152.

[75] L. H. U. Andersson, T. Hjertberg, *Polymer* **2006**, *47*, 200.

[76] J. Z. Liang, Q. Q. Yang, *J. Thermoplast. Composite Mater.* **2007**, *20*, 225.

[77] C. Remili, M. Kaci, A. Benhamida, S. Bruzaud, Y. Grohens, *Polym. Degrad. Stab.* **2011**, *96*, 1489.

[78] C. Abeykoon, M. McAfee, K. Li, P. J. Martin, A. L. Kelly, *J. Mater. Process. Technol.* **2011**, *211*, 1907.

[79] J. Liu, M. Zhang, L. Guan, C. Wang, L. Shi, Y. Jin, C. Han, J. Wang, Z. Han, *Polym. Test.* **2021**, *100*, 107236.

[80] M. Suparno, K. D. Dolan, P. K. W. Ng, J. F. Steffe, *J. Food Process. Eng.* **2011**, *34*, 961.

[81] K. Arisawa, R. S. Porter, *J. Appl. Polym. Sci.* **1970**, *14*, 879.

[82] S. R. Lim, Z. M. Ariff, W. S. Chow, *J. Thermoplast. Composite Mater.* **2014**, *27*, 1097.

[83] M. Triantou, N. Todorova, T. Giannakopoulou, T. Vaimakis, C. Trapalis, *Polym. Int.* **2017**, *66*, 1716.

[84] J. Tocháček, J. Jančář, J. Kalfus, P. Zbořilová, Z. Buráň, *Polym. Degrad. Stab.* **2008**, *93*, 770.

[85] L. Botta, F. P. La Mantia, M. Ceraulo, M. C. Mistretta, *Polym. Degrad. Stab.* **2020**, *181*, 109321.

[86] C. Freymond, A. Guinault, C. Charbuillet, B. Fayolle, *Polym. Test.* **2022**, *106*, 107458.

[87] Abohashima H. S., Aly M. F., Mohib A., Attia H. A., *Ind. Eng. Manag.* **2015**.

[88] H. Shin, E.-S. Park, *J. Polym.* **2013**, *2013*, 1.

[89] D. D. P. Moreno, C. Saron, *Waste Manag. Res.* **2018**, *36*, 729.

[90] H. Shokoohi, K. Boniface, M. McCarthy, T. Khedir Al-Tiae, M. Sattarian, R. Ding, Y. T. Liu, A. Pourmand, E. Schoenfeld, J. Scott, R. Shesser, K. Yadav, *Ann. Emerg. Med.* **2013**, *61*, 198.

[91] Y. Ding, C. Abeykoon, Y. S. Perera, *Adv. Ind. Manuf. Eng.* **2022**, *4*, 100067.

[92] M. A. Al-Saleh, A. A. Yussuf, S. Al-Enezi, R. Kazemi, M. U. Wahit, T. Al-Shammari, A. Al-Banna, *Materials* **2019**, *12*, 3924.

[93] J. Yang, G. Ding, Z. Wang, J. Gao, *J. Reinf. Plast. Compos.* **2015**, *34*, 1871.

[94] Y. Shang-Guan, F. Chen, Q. Zheng, *Sci. China Chem.* **2012**, *55*, 698.

[95] P. Gijsman, R. Fiorio, *Polym. Degrad. Stab.* **2023**, *208*, 110260.

[96] C. Maier, T. Calafut, *Polypropylene*, Vol. 3, Elsevier, Amsterdam **1998**, pp. 268–372.

[97] L. Cabernard, S. Pfister, C. Oberschelp, S. Hellweg, *Nat. Sustain.* **2022**, *5*, 139.

**ADVANCED
SCIENCE NEWS**

www.advancedsciencenews.com

**ADVANCED
ENGINEERING
MATERIALS**

www.aem-journal.com

[98] S. R. Ahmad, R. J. Young, I. A. Kinloch, *Int. J. Chem. Eng. Appl.* **2015**, *6*, 1.

[99] M. El Achaby, F. E. Arrakhiz, S. Vaudreuil, A. El Kacem Qaiss, M. Bousmina, O. Fassi-Fehri, *Polym. Compos.* **2012**, *33*, 733.

[100] I. M. Maafa, *Polymers* **2021**, *13*, 1.

[101] T. M. Akintola, P. Tran, C. Lucien, T. Dickens, *J. Compos. Mater.* **2020**, *54*, 3181.

[102] E. Malewska, A. Sabanowska, J. Polaczek, A. Prociak, *E-Polymers* **2012**, *12*.

[103] D. D. S. Rosa, F. Gaboardi, C. D. G. F. Guedes, M. R. Calil, *J. Mater. Sci.* **2007**, *42*, 8093.

[104] L. Poh, Q. Wu, Y. Chen, E. Narimissa, *Rheol. Acta* **2022**, *61*, 701.

[105] D. Li, L. Zhou, X. Wang, L. He, X. Yang, *Materials* **2019**, *12*, 1746.

[106] A. Scoppio, D. Cavallo, A. J. Müller, D. Tranchida, *Polym. Test.* **2022**, *113*, 107656.

[107] Y. Kong, J. N. Hay, *Eur. Polym. J.* **2003**, *39*, 1721.

[108] F. Al-Attar, M. Alsamhan, A. Al-Banna, J. Samuel, *J. Mater. Sci. Chem. Eng.* **2018**, *06*, 32.

[109] Q. Beuguel, S. A. E. Boyer, D. Settipani, G. Monge, J. Haudin, B. Vergnes, E. Peuvrel-disdier, Q. Beuguel, S. A. E. Boyer, D. Settipani, G. Monge, J. Haudin, **2018**, https://onlinelibrary.wiley.com/doi/abs/10.1002/pcr2.10024.

[110] A. Chafidz, M. Kaavessina, S. Al-Zahrani, M. N. Al-Otaibi, *J. Polym. Res.* **2014**, *21*, 483.

[111] M. Ajorloo, M. Fasihi, M. Ohshima, K. Taki, *Mater. Des.* **2019**, *181*, 108068.

[112] J. P. Abdou, K. J. Reynolds, M. R. Pfau, J. Van Staden, G. A. Braggin, N. Tajaddod, M. Minus, V. Reguero, J. J. Vilatela, S. Zhang, *Polymer* **2016**, *91*, 136.

[113] K. Kalaitzidou, H. Fukushima, P. Askeland, L. T. Drzal, *J. Mater. Sci.* **2008**, *43*, 2895.

[114] F. Giordano, A. Rossi, I. Pasquali, R. Bettini, A. Frigo, A. Gazzaniga, M. E. Sangalli, V. Mileo, S. Catinella, *J. Therm. Anal. Calorim.* **2003**, *73*, 509.

[115] Economic and Social Council, *Economic and Social Council* **2023**, 1.

[116] S. Snowden, 300-Mile Swim Through The Great Pacific Garbage Patch Will Collect Data On Plastic Pollution, Frobes, **2019**.

[117] R. A. Muñoz Meneses, G. Cabrera-Papamija, F. Machuca-Martínez, L. A. Rodríguez, J. E. Diosa, E. Mosquera-Vargas, *Heliyon* **2022**, *8*, e09028.

[118] I. Koswatte, J. Iddawala, R. Kulasekara, P. Ranaweera, C. H. Dasanayaka, C. Abeykoon, *Clean. Energy Syst.* **2024**, *8*, 100126.

[119] C. Abeykoon, A. McMillan, C. H. Dasanayaka, X. Huang, P. Xu, *Int. J. Lightweight Mater. Manuf.* **2021**, *4*, 434.

[120] R. Scaffaro, L. Botta, A. Maio, M. C. Mistretta, F. P. La Mantia, *Materials* **2016**, *9*, 351.

[121] E. Narimissa, R. K. Gupta, H. J. Choi, N. Kao, M. Jollands, *Polym. Compos.* **2012**, *33*, 1505.

[122] C. Gonçalves, A. Pinto, A. V. Machado, J. Moreira, I. C. Gonçalves, F. Magalhães, *Polym. Compos.* **2018**, *39*, E308.

[123] M. Wang, X. Y. Deng, A. K. Du, T. H. Zhao, J. B. Zeng, *RSC Adv.* **2015**, *5*, 73146.

[124] Y. Gao, O. T. Picot, E. Bilotti, T. Peijs, *Eur. Polym. J.* **2017**, *86*, 117.

[125] P. Cataldi, A. Athanassiou, I. S. Bayer, *Appl. Sci.* **2018**, *8*, 1438.

[126] C. Vallés, A. M. Abdelkader, R. J. Young, I. A. Kinloch, *Faraday Discuss.* **2014**, *173*, 379.

[127] G. Carotenuto, S. De Nicola, M. Palomba, D. Pullini, A. Horsewell, T. W. Hansen, L. Nicolais, *Nanotechnology* **2012**, *23*, 485705.

[128] L. Wang, J. Hong, G. Chen, *Polym. Eng. Sci.* **2010**, *50*, 2176.

[129] K. Sever, I. H. Tavman, Y. Seki, A. Turgut, M. Omastova, I. Ozdemir, *Composites, B* **2013**, *53*, 226.

[130] K. Kalaitzidou, H. Fukushima, L. T. Drzal, *Carbon* **2007**, *45*, 1446.

[131] B. Ahmadi-Moghadam, M. Sharafimasooleh, S. Shadlou, F. Taheri, *Mater. Des.* **2015**, *66*, 142.

[132] A. S. Fayed, K. A. Abu-Hasel, S. M. Mahdy, A. A. Ali, *Polym. Compos.* **2021**, *42*, 1462.

[133] E. Watt, M. A. Abdelwahab, M. R. Snowdon, A. K. Mohanty, H. Khalil, M. Misra, *Sci. Rep.* **2020**, *10*, 10714.

[134] S. H. Lee, C. R. Oh, D. S. Lee, *Nanomaterials* **2019**, *9*, 389.

[135] A. Oyarzabal, A. Cristiano-Tassi, E. Laredo, D. Newman, A. Bello, A. Etxeberría, J. I. Eguiazabal, M. Zubitur, A. Mugica, A. J. Müller, *J. Appl. Polym. Sci.* **2017**, *134*, app.44654.

[136] A. Kiziltas, W. Liu, S. Tamrakar, D. Mielewski, *Composites, Part C: Open Access* **2021**, *6*, 100177.

[137] M. Hamidinejad, B. Zhao, A. Zandieh, N. Moghimian, T. Filleter, C. B. Park, *ACS Appl. Mater. Interfaces* **2018**, *10*, 30752.

[138] J. Yu, J. E. Cha, S. Y. Kim, *Composites, B* **2017**, *110*, 171.

[139] S. Araby, Q. Meng, L. Zhang, H. Kang, P. Majewski, Y. Tang, J. Ma, *Polymer* **2014**, *55*, 201.

[140] D. Wijerathne, Y. Gong, S. Afroj, N. Karim, C. Abeykoon, *Int. J. Lightweight Mater. and Manuf.* **2023**, *6*, 117.

[141] X. Y. Qi, D. Yan, Z. Jiang, Y. K. Cao, Z. Z. Yu, F. Yavari, N. Koratkar, *ACS Appl. Mater. Interfaces* **2011**, *3*, 3130.

[142] S. V. Polschikov, P. M. Nedorezova, A. N. Klyamkina, A. A. Kovalchuk, A. M. Aladyshev, A. N. Shchegolikhin, V. G. Shevchenko, V. E. Muradyan, *J. Appl. Polym. Sci.* **2013**, *127*, 904.

[143] P. Pereira, D. P. Ferreira, J. C. Araújo, A. Ferreira, R. Fangueiro, *Polymers* **2020**, *12*, 2189.

[144] B. Mayoral, G. Menary, P. Martin, G. Garrett, B. Millar, P. Douglas, N. Khanam, M. A. AlMaadeed, M. Ouederni, A. Hamilton, D. Sun, *Front. Mater.* **2021**, *8*, https://doi.org/10.3389/fmats.2021.687282.

[145] Z. Al-Maqdasi, G. Gong, B. Nyström, N. Emami, R. Joffe, *Materials* **2020**, *13*, 2089.

[146] B. Wölfel, A. Seefried, V. Allen, J. Kaschta, C. Holmes, D. W. Schubert, *Polymers* **2020**, *12*, 1917.

[147] K. M. Bataineh, *Adv. Civil Eng.* **2020**, *2020*, 1.

[148] G. Bumanis, P. P. Argalis, G. Sahmenko, D. Mironovs, S. Rucevskis, A. Korjakins, D. Bajare, *Recycling* **2023**, *8*, 19.

[149] N. Gandhi, N. Farfaras, N. H. L. Wang, W. T. Chen, *J. Renewable Mater.* **2021**, *9*, 1463.

[150] S. Montava-Jorda, D. Lascano, L. Quiles-Carrillo, N. Montanes, T. Boronat, A. V. Martinez-Sanz, S. Ferrandiz-Bou, S. Torres-Giner, *Polymers* **2020**, *12*, 174.

[151] L. V. García-Barrera, D. L. Ortega-Solís, G. Soriano-Giles, N. Lopez, F. Romero-Romero, E. Reinheimer, V. Varela-Guerrero, M. F. Ballesteros-Rivas, *A Recycling Alternative for Expanded Polystyrene Residues Using Natural Esters*, **2022**.

[152] A. A. Alabi, L. C. Chinaza, K. A. Salami, B. O. Samuel, M. U. Suleiman, *Clean. Waste Syst.* **2022**, *3*, 100044.

[153] M. K. Eriksen, K. Pivnenko, M. E. Olsson, T. F. Astrup, *Waste Manag.* **2018**, *79*, 595.

[154] W. Tiancheng Wei, Y. Sun, E. Shim, in *Next-Generation Textiles* (Ed: H. Ibrahim), IntechOpen, Rijeka **2023**, Ch. 4.

[155] H. Jin, J. Gonzalez-Gutierrez, P. Oblak, B. Zupancic, I. Emri, in *Annual Technical Conf. - ANTEC, Conf. Proceedings,* Cincinnati, OH, April **2013**, Vol. 2, p. 967.

[156] R. Singh, N. Singh, F. Fabbrocino, F. Fraternali, I. P. S. Ahuja, *Composites, B* **2016**, *105*, 23.

[157] J. Zhang, V. Hirschberg, D. Rodrigue, *Recycling* **2023**, *8*, 2.

[158] V. Ramesh, M. Biswal, S. Mohanty, S. K. Nayak, *Waste Manag. Res.* **2014**, *32*, 379.

[159] K. Ragaert, L. Delva, K. Van Geem, *Waste Manag.* **2017**, *69*, 24.